Marine Chemistry 228 (2021) 103915

Contents lists available at ScienceDirect

Marine Chemistry

journal homepage: www.elsevier.com/locate/marchem

Riverine and wet atmospheric nutrient inputs to the Southwestern Mediterranean region of North Africa

Makhlouf Ounissi [a,*], Hadjer Laskri [a], Omar Ramzi Ziouch [a,b], Dubravko Justić [c]

[a] Laboratory of Biogeochemical and Ecological Analyses of Aquatic Environments, Department of Marine Science, University Badji Mokhtar, PO Box 12, Sidi-Amar 23005, Algeria
[b] Department of Ecology and Environment, Faculty of Science, University Abbes Laghrour, Khenchela, PO Box 1252, El Hamma 40004, Algeria
[c] Department of Oceanography and Coastal Sciences, College of the Coast and Environment, Louisiana State University, Baton Rouge, LA 70803, USA

ARTICLE INFO

Keywords:
Nutrients
Atmospheric deposition
River input
Annaba Bay
Mediterranean Sea

ABSTRACT

This study describes the first simultaneous long-term effort to examine the nutrient inputs to the southern Mediterranean Sea from rivers and wet atmospheric deposition. Extensive daily rainwater sampling (280 samples) from the Annaba region (SW Mediterranean Sea, Algeria) and from river discharges (144 samples) at two river outlets feeding the Annaba Bay, the Seybouse River (SR) and the Mafragh River (MR),were collected and analyzed for dissolved nutrients from 2012 until 2017. During the 6-year study period, the Annaba region experienced contrasted hydrological conditions varying from heavy rainfall events during winter that have triggered large river flooding in 2012 and 2015 to the severe drought of 2016, which have profoundly affected both the atmospheric and riverine freshwater and nutrient inputs. The annual freshwater volume delivered to Annaba Bay averaged approximately 1.7 km^3, of which 51% was from MR, 33% from SR, and 16% from precipitation. Precipitation over the Annaba region was associated with unusually high levels of DIP and DSi, resulting in deposition rates (0.54 mmol Si m^{-2} $yr^{-1}$and 6.22 mmol P m^{-2} yr^{-1}, respectively) that are several times higher compared to the average values reported for the Mediterranean region. In contrast, both the DIN and DON deposition rates were relatively low (16.2 and 4.7 mmol N m^{-2} yr^{-1}, respectively) compared to the values reported for the Mediterranean region. Interestingly, the levels of nitrogen compounds in rainwater were similar to those in the MR waters. For all nutrient species analyzed in this study, SR waters always contained higher nutrient levels compared to those in MR and rainwater. The majority of nutrient loading entering Annaba Bay was delivered through the riverine inputs, averaging 2744, 962 and 92 t yr^{-1} for DSi, DIN and DIP, respectively. The wet atmospheric deposition contributed only 2.5% of DSi, 10% of DIN and 7% of DIP total annual flux. The riverine stoichiometric N:P and Si:N ratios were imbalanced in most cases, averaging 28 and 0.84, respectively. The N:P and Si:N ratios in rainwater were more balanced, particularly during the dry season when Saharan airflow dominated the region and supplied more DIP and DSi.

1. Introduction

The south Mediterranean region of North Africa is a transition zone under the influence of both the temperate mid-latitude climate and the hot-dry North-African climate (Peixoto et al., 1982; Lionello et al., 2014; Ulbrich et al., 2012). These climate interactions and feedbacks between land-sea-atmosphere processes play a crucial role in shaping the hydrological cycle. Intense weather events (e.g., heavy rains, winds, floods, droughts, and frequent Saharan dust events) commonly affect the region (Lionello et al., 2014; Gaume et al., 2016). However, torrential river flows are common during heavy rains that occur primarily during autumn and winter (Struglia et al., 2004; Tarolli et al., 2012; Xoplaki et al., 2014). In this region, over 80% of the annual precipitation yield occurs during winter (October-March), while summer season typically exhibits drought and arid conditions (Peixoto et al., 1982; Ulbrich et al., 2012). Consequently, the maximum river discharges also occur during October-March period (Guerzoni et al., 1999; Skoulikidis et al., 2016).

The North African rivers generally carry high nitrogen (N), phosphorus (P) and silica (Si) loads, in response to natural (e.g., weathering and soil erosion) and anthropogenic factors (e.g., untreated wastewater, agricultural fertilizer use) (Ounissi and Bouchareb, 2013; Ounissi et al., 2014; Tovar-Sánchez et al., 2016). Over the past several decades, the N

* Corresponding author.
E-mail addresses: makhlouf.ounissi@univ-annaba.dz (M. Ounissi), djusti1@lsu.edu (D. Justić).

https://doi.org/10.1016/j.marchem.2020.103915
Received 24 June 2020; Received in revised form 22 September 2020; Accepted 11 December 2020
Available online 17 December 2020

and P fluxes from the Mediterranean rivers may have increased by more than 5-fold and 3-fold, respectively (Ludwig et al., 2009). These high nutrient loads, besides sustaining the high productivity of coastal waters (Maavara et al., 2014; Macias et al., 2017), also promote eutrophication that is often manifested in noxious and harmful algal blooms, hypoxia, degradation of pelagic and benthic habitats, and changes in the structure of coastal food webs (Cloern, 2001; Duce et al., 2008; Galloway et al., 2008).

In addition to N and P, Si plays a crucial role in controlling diatom abundance and the overall structure of coastal food webs. Diatoms need Si to build their external frustules, and their growth generally becomes Si-limited when Si:N molar ratio falls below 1:1 (Justić et al., 1995; Yool and Tyrrell, 2003). In contrast to the increasing trends in riverine N and P delivery, the levels of dissolved Si have dramatically decreased in many coastal regions worldwide (Conley et al., 2000; Humborg et al., 2000). Importantly, N and P sequestration in reservoirs can be counterbalanced by human activities, but there is no similar compensation for Si (Conley et al., 2000; Friedl and Wüest, 2002; Maavara et al., 2014). The decline in Si transport to the coastal ocean can in turn change the ratio of nutrients available for phytoplankton growth and thus affect the coastal food webs (Turner et al., 1998; Humborg et al., 2000; Cozzi et al., 2018).

In addition to riverine nutrient loadings, numerous studies conducted along the Mediterranean Sea, encompassing both coastal and open waters, have pointed out that the atmospheric deposition is a significant source of nutrients (Herut et al., 1999; Markaki et al., 2010; Koçak et al., 2010; Violaki et al., 2010; Christodoulaki et al., 2016). Moreover, due to its close proximity to the Saharan arid region, the Mediterranean Sea receives large quantities of mineral dust (Loÿe-Pilot et al., 1986; Guerzoni et al., 1999; Kubilay et al., 2000; Prospero et al., 2002; Ridame and Guieu, 2002; Rogora et al., 2004; Prospero, 2014), which delivers soluble N, P, Si and other micronutrients (Bonnet et al., 2005; Barkley et al., 2019). In recent years, the North African Saharan dust episodes and associated transport over the western Mediterranean regions have become more frequent, which not only constitutes an important source of nutrients but also contributes significantly (with their alkaline pH and high acid-neutralizing capacity) towards buffering the mineral acidity of rainwater (Rogora et al., 2004; Morales-Baquero et al., 2013). Also, wet deposition was found to be the main factor controlling dissolved inorganic nitrogen (DIN) and dissolved inorganic phosphorus (DIP) depositions in the Mediterranean Sea, especially during the wet season (Markaki et al., 2010). Biomass burning aerosol was also found to be an important atmospheric source of nutrients for the Mediterranean Sea (Guieu et al., 2005).

The atmospheric N deposition to the Mediterranean Sea has been estimated to be comparable(or even higher in some regions) to the riverine N input (Martin et al., 1989; Loÿe-Pilot et al., 1990), and is therefore expected to strongly influence the regional N budgets (Guerzoni et al., 1999; Ridame and Guieu, 2002; Markaki et al., 2003; Christodoulaki et al., 2016). Atmospheric N deposition may account for up to 35–60% of new production in the Mediterranean open waters (Christodoulaki et al., 2013), particularly during the period of stratification (summer and autumn). Atmospheric P deposition is also important (Bergametti et al., 1992) and can account for 20–30% of the new primary production in the Eastern Mediterranean and 22–40% in the Levantine Sea (Markaki et al., 2003). Most of the studies of atmospheric nutrient deposition to the Mediterranean coastal and open waters have focused on DIP and DIN, while a few studies have also considered Si deposition (Koçak et al., 2010; Desboeufs et al., 2018).

A number of recent studies recognized that DON is a ubiquitous component in atmospheric deposition, contributing to ~30% of the total dissolved nitrogen (TDN) (Neff et al., 2002; Cornell, 2011; Cape et al., 2012; Kanakidou et al., 2012; Li et al., 2012; Kanakidou et al., 2018), that plays an important role in sustaining phytoplankton growth and N cycling. Yet, very few studies in the Mediterranean region have provided information on the DON levels and deposition (e.g., Mace et al. (2003), Violaki et al. (2010), Nehir and Koçak (2018) for the E Mediterranean, and Djaoudi et al. (2018) for NW Mediterranean). Moreover, riverine and atmospheric DON inputs to the SW Mediterranean region have never been systematically evaluated.

A number of studies have been carried out to quantify fluxes of nutrients from riverine or atmospheric inputs, mainly in the Northern and Eastern Mediterranean, but with the exception an annual survey by Ounissi et al. (2018) there are no contemporaneous data on riverine and atmospheric inputs to the Southwestern Mediterranean. To our knowledge, the review of Martin et al. (1989) and the study of Koçak et al., 2010 (Northeastern Mediterranean) are the only works that concurrently assessed the riverine and atmospheric nutrient inputs. Despite the importance and the quality of data provided in these works, DON and Si are not included in the review of Martin et al. (1989) and DON is not considered in Koçak et al. (2010). Because rainfall and river discharges strongly differ among the coastal and open Mediterranean regions, it is important to develop complete nutrient inventories for each specific region.

Annaba Bay (Southwestern Mediterranean, Northeastern Algeria) is a singular coastal ecosystem receiving freshwater discharges from two important rivers in North Africa, namely the Seybouse and Mafragh Rivers. The two river catchments (10,000 km^2) host around 1.5×10^6 inhabitants and deliver collectively approximately 1.3 $km^3\ yr^{-1}$ of freshwater, heavily loaded with various terrestrial materials and pollutants (Ounissi et al., 2014; Ounissi et al., 2018). The Annaba region is characterized by a humid climate and receives an annual precipitation yield of 400–800 mm (Ounissi et al., 2018). The region is strongly influenced by the Saharan dust inputs, which typically occur from March until October (Salvador et al., 2014; Varga et al., 2014).

As stated above, despite a few published works on the Seybouse and Mafragh Rivers (Ounissi et al., 2014, 2016, 2018; Ziouch et al., 2020) and other contiguous rivers (Ounissi and Bouchareb, 2013), the data on nutrient fluxes from Algerian rivers are still lacking. This study describes the first contemporaneous long-term effort (2012–2017) to examine the nutrient inputs to Annaba Bay from rivers and wet atmospheric deposition. The objectives are to (i) assess and compare nutrient inputs to Annaba Bay from riverine and atmospheric sources, (ii) explore seasonal and inter-annual variability in nutrient inputs from riverine and wet atmospheric deposition, and, (iii) fill the gaps in freshwater discharge and nutrient input inventories (DON and Si in particular) for the Southwestern Mediterranean Sea.

2. Materials and methods

2.1. Sampling sites

Annaba Bay is a particular coastal area of the Southwestern Mediterranean Sea (Northeastern Algeria, Fig. 1), with an exceptionally large drainage area/bay area ratio of 25. The bay receives freshwater discharges mainly from the Seybouse River and the Mafragh River. From the land side, the bay is also influenced by discharges from a large fertilizer factory (Fertial) (Frehi et al., 2007; Ounissi et al., 2014; Ounissi et al., 2016), as well as wastewaters from Annaba city and its surrounding villages (about 1.2×10^6 inhabitants). From the ocean side, the bay is subjected to the intrusions of the modified Atlantic water, which modifies the continental inputs (Ounissi and Frehi, 1999; Ounissi et al., 1998), particularly during the periods of intense mixing (October–March). Regarding the atmospheric forcing, the Annaba region is mostly influenced by two contrasting air masses, the cold and humid airflow originating from Europe (October–March) and the warm and dry airflow originating from the African desert (April–September). The Annaba region receives 460–820 mm yr^{-1} in precipitation (Mehta and Yang, 2008), with a maximum during November–January. Storm frequency is the highest during the spring (April–May) and fall (August–September) periods.

During the extended dry period (April–September), the region is

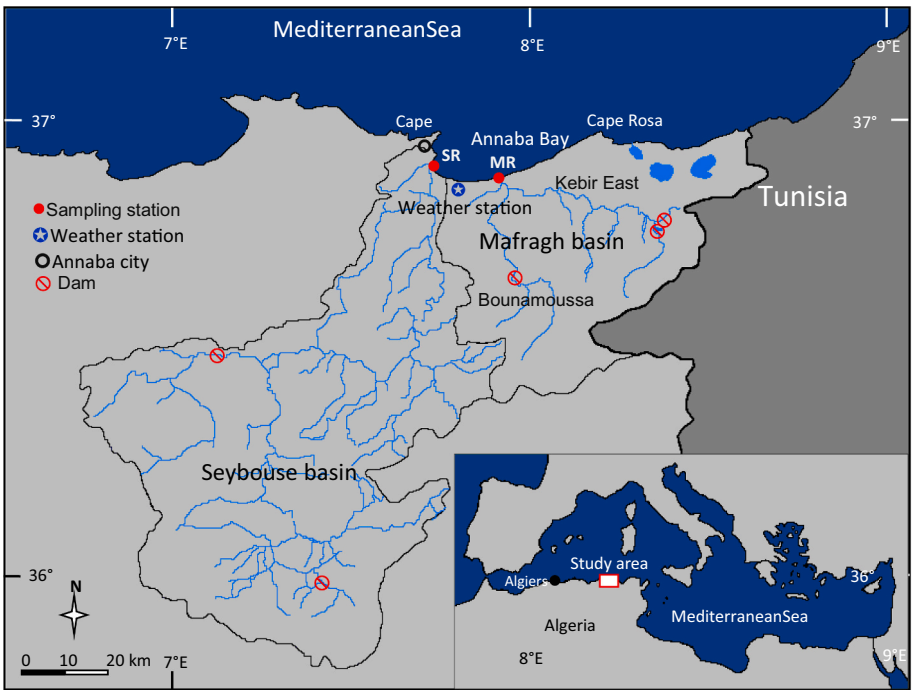

Fig. 1. Map of the Seybouse and Mafragh River catchments and their adjacent coast (Annaba Bay). The locations of weather and sampling stations are also shown; SR-Seybouse River outlet; MR-Mafragh River outlet.

subjected to high levels of dust deposition from the adjoining Algerian desert (Morales-Baquero et al., 2013; Salvador et al., 2014; Varga et al., 2014; Vincent et al., 2016). The northern and southern Algeria have been identified as the main potential source areas of African dust transport to the western Mediterranean basin (Salvador et al., 2014). Dust transport from these areas occurs in summer and autumn, respectively. In addition, the northeastern Algeria and Tunisia (some tens km south/south east Annaba coast, NE Algeria) contributed to the dust transport both in spring and summer (Salvador et al., 2014).

With an annual mean precipitation of 740 mm, the Mafragh watershed is considered to be among the wettest areas in Algeria (Philandras et al., 2011; UNEP/MAP, 2013). The resulting runoff is intercepted by a series of three dams (total storage capacity of 300 $\times$ 10^6 m^3) and a large flood plain containing marshlands (about 170 km^2). The mean discharge at MR outlet is only 24 m^3 s^{-1} (UNEP/MAP, 2013). However, the MR discharge can vary significantly from over 2000 m^3 s^{-1} during the peak flows to zero during the extended dry period. Indeed, the MR outlet is disconnected from the adjacent ocean for several months (usually during June-November), due to the dam retention and unregulated water use (Khélifi-Touhami et al., 2006; Ounissi et al., 2014). In addition, the microtidal regime of the estuary (tidal range ~ 20 cm) facilitates the closing of the MR outlet. The MR has a large brackish section (20 km in Kebir East branch and 8 km in Bounamoussa branch), which typically occurs during March-May, following the December-February peak in freshwater discharge (Khélifi-Touhami et al., 2006; Ounissi et al., 2014). The MR watershed is mostly forested (57.3%) while agricultural areas in the middle and lower sections occupy about 25% of the watershed, although the area is sparsely populated (about 0.5 $\times$ 10^6 inhabitants). Another notable characteristics of the MR catchment is the presence of multiple successive water bodies (the so-called cascading filters, Viaroli et al., 2015) along the aquatic continuum (reservoirs, wetlands, marchlands and a large brackish section), which can retain nutrients and other materials.

The Seybouse River system (240 km length) functions as a river-estuary. Tidal intrusion is pronounced in its lowermost part (8 km) throughout the dry period (April-September), promoting the development of a strongly stratified system with a prominent saltwater wedge below a thin brackish surface layer (Ounissi et al., 2014; Ziouch et al., 2020). During the wet period (October–March), the SR intermittently runs fresh for several days/weeks (after heavy rains), causing the retreat of the salt wedge back to the coast. The SR watershed is considered to be among the most developed river systems in Algeria (Ounissi et al., 2014, 2018; Ziouch et al., 2020). Here, irrigated land and intensive agriculture have encompassed some 4% of the total catchment area (UNEP/MAP, 2013), predominantly in the middle and lower sections of the basin. As a result, large quantities of surface water (400 million m^3) have been retained in dams to fulfill irrigation needs. Moreover, most of the domestic waste of the population (1.5 $\times$ 10^6 inhabitants) is directly delivered into the watershed network. The lower catchment (about 10 km from the coast) is also heavily populated and receives various industrial pollutants (agro-food, metal steel, milk products, pharmaceutics, and numerous other small industries).

2.2. Analytical methods

2.2.1. Riverine water sampling and chemical analyses

The water discharge measurements and nutrient analyses were carried out from January 2012 until December 2017. The sampling protocol was rather heterogeneous, with the sampling frequency varying from twice a day during the flood of 2015 (28 February–18 March 2015), weekly during 2014, fortnightly during 2012 to monthly during 2013, 2015, 2016 and 2017. A total of 291 samples were collected, 150 at the MR outlet and 141 at the SR outlet. Of the two large flood events that occurred during the study period (late February 2012 and late February–mid March 2015), the flood of 2015 was extensively sampled from the peak discharge period (28 February) until the discharge declined to the base flow (16 March). However, we provide here only the monthly mean values to facilitate the long-term time-series presentation.

During the course of sampling, we assessed the freshwater flow velocity from the outlet' stations of the SR and MR estuaries with CM-2 current meter (Toho Dentan Co., Ltd., Tokyo). The freshwater discharge (m^3 s^{-1}) was calculated by multiplying the water velocity (m s^{-1}) with the total surface area (m^2) of the estuary's transect.

Measurements of water velocity were taken at several points depending on the estuary section width and depth. This allowed computing the average current velocity. The freshwater layer was determined for each sampling date (see Ziouch et al., 2020). Water samples (2 L from the surface freshwater layer) for nutrient analyses were frozen in polyethylene bottles and processed within two days from collection. They were analyzed for dissolved nitrogen (NH_4, ammonium; NO_3, nitrate; NO_2, nitrite; DON: dissolved organic nitrogen), phosphate (PO_4, herein referred to as DIP) and silicate ($Si(OH)_4$, herein referred to as DSi) following the manual methods described in Parsons et al. (1989). The respective accuracies of analytical methods were as follows: PO_4: ± 3.4%; NH_4: ± 3.3%; NO_3: ± 2.6%; NO_2: ± 3.7%; $Si(OH)_4$: ± 1.2%; DON: ± 5.5%. Measurements of salinity (practical salinity scale: pss) were performed in situ using a Multi-parameter WTW Cond1970i. All the analyses, with the exception of pH and salinity, were performed on filtered samples (0.45 μm micropore filters). The hydrological measurements used in this study utilized the same methods as described in Ziouch et al. (2020) and Ounissi et al. (2014).

The annual fluxes for dissolved nutrients were estimated using the method of average instantaneous loads (Preston et al., 1989). Details on flux estimation are provided in Ounissi et al. (2014). For the 2015 flood (28 February–18 March) the fluxes of water and nutrients were estimated from daily means of all samples using the volume weighted mean concentration/flow (VWM; 38 samples for MR, sampled twice a day from 28 February–18 March; 17 samples for SR, sampled daily from 1 to 17 March). Only a brief account of this particular flooding event is given here; a detailed analysis will be presented in the forthcoming paper. To facilitate comparisons between the MR and SR catchments, the fluxes (tons per year, t yr^{-1}) were normalized by the respective catchment area and expressed in tons per square kilometer per year (t km^{-2} yr^{-1}).

2.3. Rainwater water sampling, nutrient analyses and deposition estimation

The rainwater collection was performed using a rainfall collector (200-cm^2 cross-sectional area) housed in a fenced area at the Annaba weather station (36°49′19″N, 7°48′11″E), located 3 km from the Annaba Bay (Fig. 1). Rainwater was sampled after each rainfall event in order to prevent microbial nutrient transformations. The Annaba weather station is well within the reach of pollutants from municipal and industrial sources, e.g., 10 km from Annaba city and its neighboring agglomerations (about 1 million inhabitants), 5 km from a large fertilizer factory (Fertial), and about 10 km from a the industrial steel complex of El Hadjar. In particular, the fertilizer factory is known for its large emissions of ammonia.

Table 1 summarizes the annual precipitation characteristics for the Annaba region during the 2012–2017 study period, and gives the breakdown of sampling effort by months and year. Out of 584 rain days recorded during the 2012–2017 study period, 280 daily rainwater samples (48%) were collected and analyzed (SI, sheet 2). The number of samples collected each month has varied considerably depending on the season and year, from 3 to 8 samples during the dry period (May–August) to 33–52 samples during the wet period (November–February).

The collected rainwater samples were transferred into 2 L polyethylene bottles, transported to the laboratory, filtered and analyzed during the same or the following day. Similarly to the river water samples, the rainwater samples were analyzed for the pH and dissolved nutrients (NH_4, NO_3, NO_2, DON, PO_4, $Si(OH)_4$). The dissolved inorganic nitrogen (DIN = NH_4 + NO_3 + NO_2) and total dissolved nitrogen (TDN = DIN + DON) were also calculated for each sample. About a third of the collected rainfall samples had insufficient volume for all the chemical analyses to be carried out, and those samples were diluted with distillated water to obtain the required volumes. The pH measurements were performed on unfiltered samples with the Multi-parameter WTW Cond 1970i. A total of 117 samples were analyzed for pH, of which 61 were collected during 2016 (see SI, sheet 3).

Table 1
Number of daily samples (by month) of rainwater from the Annaba region during the 2012–2017 study period. The annual sampled days and volumes of precipitation are also given.

	2012	2013	2014	2015	2016	2017	Total
January	2	11	7	7	8	17	52
February	7	9	0	6	8	3	33
March	6	4	7	3	9	1	30
April	9	2	1	0	2	5	19
May	0	1	2	1	2	0	6
June	0	0	1	2	2	3	8
July	0	0	1	0	1	1	3
August	0	3	0	2	0	1	6
September	3	2	2	7	4	2	20
October	5	0	3	8	6	6	28
November	5	6	0	10	11	9	41
December	5	4	8	2	8	7	34
Total	42	42	32	48	61	55	280
	2012	2013	2014	2015	2016	2017	Mean
Annual precipitation (mm)	536	703	595.5	760.2	463.5	650.2	618
Num. of days with rain	83	117	100	95	101	88	97
% of days sampled	50.6	35.9	32	50.5	60.4	62.5	48
Sampled volume (mm)	350.3	481.0	229.7	506.6	383.2	508.1	410
% of sampled volume	65.4	68.4	38.6	66.6	82.7	78.1	66.3

The wet atmospheric deposition fluxes (*Fw*) were estimated using the method of Herut et al. (1999). The volume weighted mean nutrient concentrations (*Cw*) in rainwater were computed from the equation:

$$Cw = \frac{\sum_{i=1}^{n} Ci \times pi}{\sum_{i=1}^{n} pi} \mathrm{Cw} = \frac{\sum_{i=1}^{n} \mathrm{CiQi}}{\sum_{i=1}^{n} \mathrm{Qi}}$$

Where *Ci* is the nutrient concentration of a given nutrient species, and *pi* is the rainfall amount for the given precipitation event. The wet deposition fluxes (*Fw*) were computed by multiplying the *Cw* values for the given nutrient species with the yearly rainfall amounts (P_{yr}):

$$Fw = Cw \times P_{yr}$$

To compare the wet atmospheric nutrient deposition (WAD) to the nutrient loads entering the Annaba Bay (herein referred to as AB) from the MR and SR outlets, the WAD values (expressed in mmol m^{-2} yr^{-1}) for the various nutrients species deposited over the AB (400 km^2) were converted to tons per year (t yr^{-1}).

3. Results

3.1. Seasonal and inter-annual variations in hydrological parameters at the rivers' outlets

Fig. 2 shows the monthly variations in precipitation over the MR and SR catchments and freshwater discharges and salinity at the river outlets during the 2012–2017 study period. For the lower SR catchment, the annual precipitation yield fluctuated between 470 mm in the dry year of 2016 and 760 mm in the wet year of 2015, with an annual mean of 620 mm. The MR catchment had a 26% higher annual rainfall (mean 784 mm) compared to SR. Overall, variations in the seasonal precipitation were similar in the two catchments, with the wet season extending from October to March and the dry season from April to September (Fig. 2). The wet season contributed 85% and 80% of the annual rainfall in the SR and MR catchments, respectively. During the 6-years study period, several heavy rainfall events occurred during winter, such as those of February 2012, November 2013, December 2014, February 2015 and November 2017 (Fig. 2). However, only the heavy rainfalls of late February 2012 and late February 2015 have triggered strong river

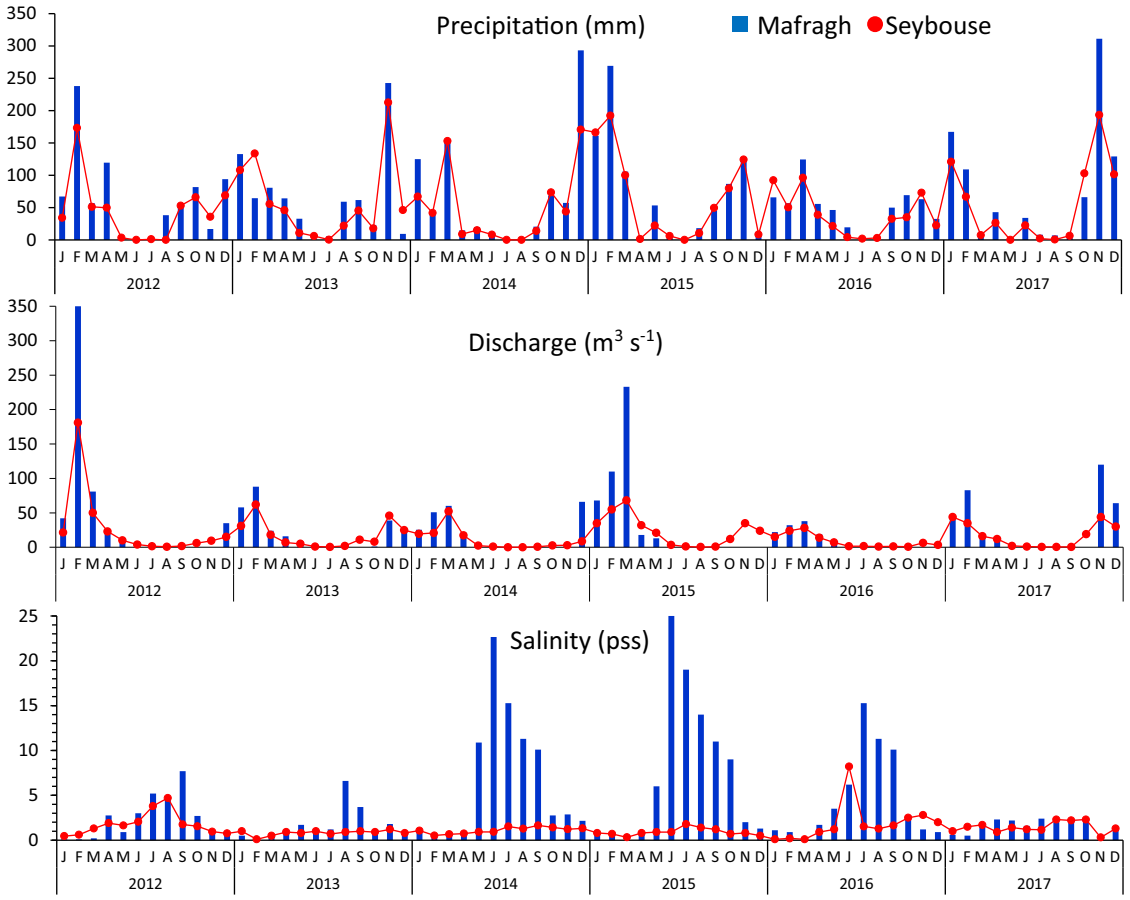

Fig. 2. Seasonal variations in precipitation, water discharge and salinity for the Seybouse and Mafragh catchments during the 2012–2017 study period. Water discharge and salinity were measured at the catchment outlets; precipitation data over the Mafragh catchment were collected at the weather station 'Lac des Oiseaux', located 16 km from the Mafragh; precipitation data for the Seybouse catchment were collected at the Annaba weather station (Fig. 1).

flooding, especially in the MR catchment (Fig. 2).

Because of the water retention behind dams in the middle and upper catchments, riverine discharges at the river outlets did not follow closely the seasonal cycle of precipitation, particularly for the MR. Also, the flow ceased for several months at the MR outlet (usually from May/June to November/December), and the estuary was disconnected from the sea during that time (Fig. 2) in response to weak tidal forcing (~ 20 cm). The lowest discharges occurred during the dry years (2014 and 2016), when a significant fraction of the flow was retained in reservoirs and used mainly for irrigation needs. The minimum discharge was recorded during the drought of 2016 (8.7 and 10 $m^3 s^{-1}$ for SR and MR, respectively) and the maximum discharge during the flood of 2012 (45 and 27 $m^3 s^{-1}$ for MR and SR, respectively). The flood of February 2012 was devastating in the MR catchment, during which an exceptionally high flow of 2100 $m^3 s^{-1}$ was recorded, and the mean monthly flow reached 350 $m^3 s^{-1}$ (Fig. 2). The flood of February–March 2015 in MR was also significant, when the maximum discharge reached 900 $m^3 s^{-1}$ and the monthly mean flow averaged 233 $m^3 s^{-1}$ (Fig. 2). The combined annual discharge of the two rivers averaged 1.4 km^3 during the 2012–2017 period, with a maximum of 2.28 km^3 during 2012 and a minimum of 0.59 km^3 during 2016 (SI, sheet 1). During the 2012–2017 study period, the annual mean freshwater volume discharged into the Annaba Bay, including the direct precipitation (mean 620 mm), was 1.65 km^3, of which the MR accounted for 51.5%, the SR 33.5% and direct precipitation for 15.0%. The highest freshwater discharge was recorded during February, followed by March, January, November and December (SI, sheet 1).

During the wet period characterized high river discharges (> 50 $m^3 s^{-1}$), surface salinity at MR and SR outlets was generally <1, reflecting typical freshwater conditions. During the dry period, when the water discharge dropped to nearly zero in the SR outlet and to zero in the MR outlet, salinity values increased to >2 (Fig. 2).

Fig. 3 shows the monthly means and variations in nutrient concentrations and stoichiometric nutrient ratios at the MR and SR outlets during the 2012–2017 study period. Regardless of the year, the total dissolved nitrogen (TDN) levels were always 2-fold to 5-fold higher at the SR outlet compared to the MR outlet. This is mainly because the SR waters were strongly enriched with ammonium, with annual mean NH_4 levels ranging from 38 to 121 μmol L^{-1} (Fig. 3).

In SR waters, NH_4 fraction of TDN ranged between 42.3% in 2014 to 82.2% in 2017. Levels of NH_4 increased throughout the dry season with the mean monthly values reaching 53–150 μmol L^{-1}, but decreased during the wet period (November-March) to 22–45 μmol L^{-1} (Fig. 3). In contrast, annual mean levels of NH_4 for MR waters were very low and ranged between 3.6 and 16 μmol L^{-1} (mean 8.5 μmol L^{-1}). NH_4 also had a different seasonal cycle with low values during the dry period (Fig. 3), reflecting the isolation of the estuarine reaches from both the continental and marine influences.

Similarly to NH_4, the annual mean nitrate (NO_3) levels in SR waters were always higher (10–31 μmol L^{-1}, mean 22.8 μmol L^{-1}) than in the MR waters (7–22 μmol L^{-1}, mean 14.5 μmol L^{-1}, Fig. 3). NO_3 concentrations in the SR and MR rivers had similar seasonal cycles (Fig. 3). However, in contrast to the SR, NO_3 fraction of TDN in the MR was higher and accounted for 1/3 to 1/2 the TDN levels, except during 2017 where the fraction of NO_3 in TDN decreased to 22% (SI, sheet 1).

The dissolved organic nitrogen (DON) concentrations showed a clear

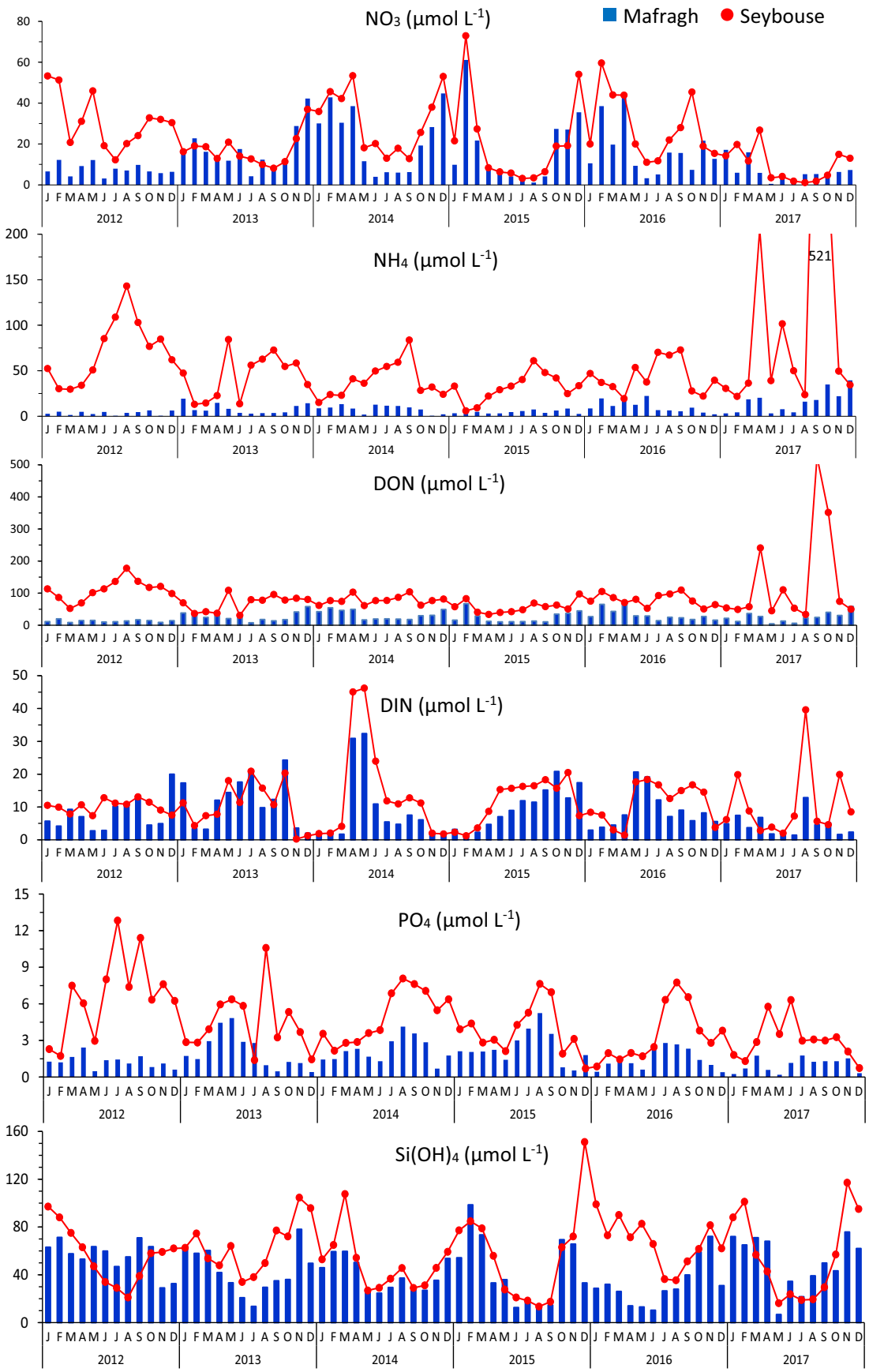

Fig. 3. Monthly variations in dissolved nutrient concentrations at the Seybouse and Mafragh River outlets during the 2012–2017 study period.

seasonal cycle (Fig. 3) with high monthly mean values during the dry season (April-October), reaching on average 15 and 11 μmol L^{-1} in SR and MR waters, respectively. These peak concentrations were 50% and 30% higher relative to the annual mean DON levels in SR and MR, respectively. However, the DON fraction in TDN averaged 25% in the MR, compared to only 12.5% in the SR, which was likely due to the higher NH_4 levels in SR. At the SR outlet, the dissolved inorganic nitrogen (DIN = $NO_3 + NO_2 + NH_4$) accounted for 87.5% of the TDN, and exhibited the same seasonal trend of the dominant NH_4 fraction. At the MR outlet, however, the DIN pattern closely mirrored the seasonal cycle of NO_3, which dominated both DIN and TDN (Fig. 3, SI, sheet 1).

The SR contained high phosphate (PO_4 = DIP) concentrations, with the annual mean DIP levels ranging from 3.06 μmol L^{-1} in 2017 to 6.7 μmol L^{-1} in 2012. The mean DIP levels in the SR were 2 to 3-fold higher than in the MR waters. DIP levels displayed a clear seasonal pattern with high values during the dry season, especially in the SR (Fig. 3). The highest DIP values in the MR were observed during the outlet closing period, which could be related to the DIP release from the sediments. During the time when the estuary was not exposed to marine or freshwater influence, the estuary was controlled vertically by the sediment-water column and groundwater exchanges and atmospheric forcing (wind mixing, evaporation).

In contrast to the high DIN and DIP concentrations, the SR and MR displayed low dissolved silicate (DSi) levels regardless of the year and the season. As shown in Fig. 3, the concentration of DSi never exceed 100 μmol L^{-1} at the MR outlet and surpassed 100 μmol L^{-1} in only four cases at the SR outlet. Compared to the DSi concentrations in the MR, the mean DSi levels in the SR were slightly higher, ranging from 48.6 μmol L^{-1} in 2014 to 67.5 μmol L^{-1} in 2016 (Fig. 3). The mean DSi values for the MR ranged from 31.7 μmol L^{-1}during a drought year (2016) to 55.5 μmol L^{-1}during the flood year (2012). In both rivers, the DSi levels exhibited a clear seasonal cycle with high values during the wet season and very low values during the dry season (Fig. 3).

Fig. 4 shows the seasonal variations in the DIN:DIP molar ratios (herein referred to as N:P) at the MR and SR outlets throughout the 6-years study period. In the SR waters, the highest ratios (> 20) occurred during the wet season (with the exception of July 2013), while most of the low values <10 occurred during the dry season (Fig. 4). At the SR outlet, the annual mean values of N:P varied between 18.8 and 49.9 (SI, sheet 1). However, a half of the samples approached the Redfield ratio (i.e., 10 < N:P < 20), and the remaining half were unbalanced (10 samples with N:P < 10 and 26 samples with N:P > 20). At the MR outlet, the annual mean N:P values ranged between 12.6 in 2012 to 39.9 in 2017. Yet, only 15 samples had balanced N:P ratios (10 < N:P < 20) and the rest of the samples (79%) showed large departure from the Redfield values (Fig. 4). Most of samples with N:P < 10 were collected during the outlet closing period and almost all of those with N:P > 20 during the months with high MR discharges.

The SR waters were characterized by very low DSi:DIN ratios (herein referred to as Si:N), with an annual mean value ranging from 0.6 to 1.0. About two-thirds of samples had lower values relative to the Redfield ratio (i.e., Si:N ~ 1) and the rest of the samples had a more balanced Si:N ratios (Fig. 4). The departure in the Si:N values from the Redfield ratio was the highest during the dry season, and the few samples with balanced Si:N ratios were collected during the high river discharges (Fig. 4). In contrast, the MR waters were characterized by high Si:N ratios, ranging on average from 1.3 to 4.4. Only 10 samples (13%) collected during the outlet closing period showed unbalanced Si:N ratios, while the rest of the samples displayed high Si:N values.

3.2. Seasonal and inter-annual variations in nutrient levels of rainwater

Variations in the monthly mean nutrient concentrations in rainwater throughout the study period are shown in Fig. 5. Additionally, daily nutrient concentrations and a summary of annual mean nutrient values and stoichiometric nutrient ratios are provided as supplementary material (SI, sheet 2). Mean annual concentrations of TDN varied over a narrow range of 33.1–40.9 μmol L^{-1}, with an overall mean of 38 μmol L^{-1}. This value is not much different (+ 16%) from the volume weighted mean (VWM) average (Table 2). The multiannual contributions of the various nitrogen components to TDN were as follow: 39.5% for NO_3, 32% for NH_4, 24.3% for DON and 4.2% for NO_2. The VWM levels were usually slightly lower than their respective arithmetic means, except for DON (16% higher) and NO_3 (13% higher, Table 2). The TDN concentration exhibited large seasonal fluctuations, with high values typically observed during the dry season (Fig. 5). The monthly mean DON values showed a clear seasonal pattern, with increased concentrations during May-July (11.7–13.2 μmol L^{-1}) and lowest values during the wet season (8–8.6 μmol L^{-1}). The only exception was September 2016 when the lowest DON value was recorded (Fig. 5, SI, sheet 2).

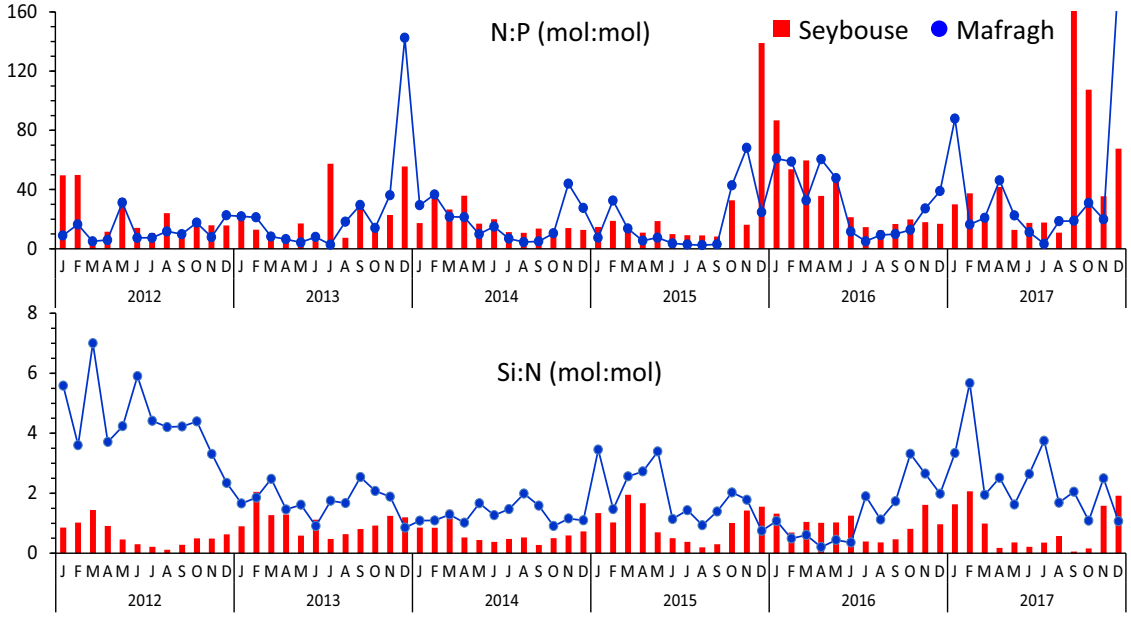

Fig. 4. Monthly variations in stoichiometric nutrient ratios (N:P and Si:N) at the Seybouse and Mafragh River outlets during the 2012–2017 study period.

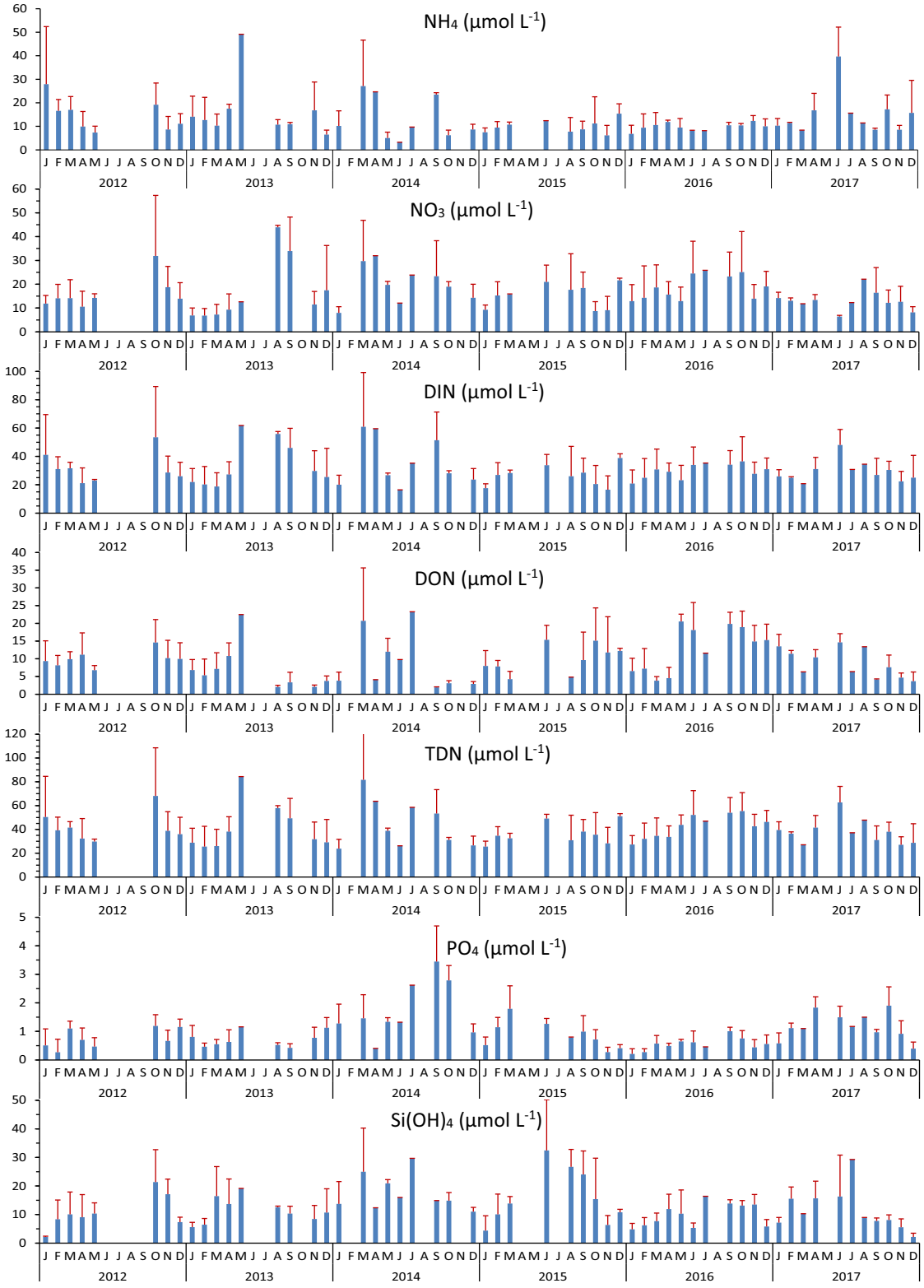

Fig. 5. Monthly means and standard deviations (red bars) of nutrient concentrations in rainwater from Annaba region during the 2012–2017 years. (For interpretation of the references to colour in this figure legend, the reader is referred to the web version of this article.)

Monthly mean NO_3 levels varied over a wide range of 10–23 µmol L^{-1}, reaching the highest values between August and October (19.4–23.1 µmol L^{-1}), when it constituted about 50% the TDN levels. The concentration of NH_4 showed no clear seasonal pattern and varied within a narrow range of 9.3–16.5 µmol L^{-1}, with an annual mean value of 12.5 µmol L^{-1}.

The DIP and DSi concentrations also showed seasonal variations (Fig. 5), with higher values during the dry season (June-October) and lower values during the wet season (November-February). The mean annual concentrations greatly varied for both DIP and DSi (SI, sheet 2). The minimum DIP concentration (0.5 µmol L^{-1}) was recorded in 2016 and the maximum in 2014 (1.5 µmol L^{-1}), with a multiyear mean of

Table 2
Annual average (A: arithmetic mean) and volume weighted mean concentration (VWM) of nutrients and their ratios (N:P = DIN:DIP; Si:N = DSi:DIN) in rainwater from the Annaba region during the 2012–2017 study period; (%) denotes a fraction of the given nitrogen species with respect to TDN.

		NH_4	NO_3	NO_2	NID	DON	TDN	DIP	DSi	N:P	Si:N
2012	A	13.8	15.9	1	30.7	10.2	40.9	0.8	11.1	86.5	0.42
	VWM	12.9	16.4	1.1	30.4	9.8	40.2	0.74	11.1	41.2	0.36
	%	(33.7)	(38.9)	(2.4)	(75.1)	(24.9)					
2013	A	13.7	12.8	1.1	27.5	5.6	33.1	0.7	9.1	63.0	0.39
	VWM	13.8	10.1	1.19	25.1	5	30.1	0.68	9.5	36.8	0.38
	%	(41.4)	(38.7)	(3.3)	(83.1)	(16.9)					
2014	A	13.9	18.4	2.3	34.6	8.4	43.0	1.5	16.7	32	0.58
	VWM	9.6	15.8	1.8	27.2	5.8	33.0	1.47	13.6	18.5	0.50
	%	(32.3)	(42.8)	(5.3)	(80.5)	(19.5)					
2015	A	9	13.2	1.2	23.4	10.3	33.8	0.8	13.5	47.5	0.78
	VWM	8.6	12.1	1.3	22	8.4	30.3	0.76	10.7	28.8	0.49
	%	(26.6)	(39.1)	(3.6)	(69.2)	(30.5)					
2016	A	10	17.5	1.3	28.8	11.8	40.7	0.5	9.1	66.5	0.38
	VWM	8.6	12.1	1.3	22	8.4	30.3	0.76	10.7	63.9	0.32
	%	(24.6)	(43.0)	(3.2)	(70.8)	(29.0)					
2017	A	13.7	12.5	1.3	27.5	9.2	36.8	1.0	8.6	41.5	0.36
	VWM	14.7	12.3	1.16	28.1	8.8	36.9	1.12	7.0	25.2	0.25
	%	(37.2)	(34.0)	(3.5)	(74.7)	(25.0)					

0.88 μmol L^{-1}. The DIP VWM levels closely followed their respective arithmetic means, except for the driest year of 2016, where the VWM value was 1.5-fold higher than the arithmetic mean. The mean annual DSi levels varied from 8.6 μmol L^{-1} in 2017 to 16.7 μmol L^{-1} in 2014, with an overall mean of 11.4 μmol L^{-1}.

The monthly mean of N:P ratios varied over a wide range of 23–54 (SI, sheet 2), but with no clear seasonal cycle. However, the N:P ratios decreased with the increasing of DIP levels (> 1 μmol L^{-1}) during June-July and September-October periods. In addition, because the mean monthly DIN levels were fairly constant, the highest N:P ratios occurred coincidentally with low DIP levels (< 0.6–0.8 μmol L^{-1}) during the wet season.

Unlike the N:P ratios, the monthly mean Si:N ratios fluctuated over a narrow range of 0.3–0.5. Generally, the Si:N ratios increased during summertime with the increasing DSi levels (SI, sheet 2). The more balanced nutrient ratios during the dry season likely occurred in response to the excess DIP and DSi loading with respect to DIN, which could be explained by the frequent Saharan dust inputs during that time. In fact, the high pH in rainfall during the dry season of 2016 (7.0) was characteristic for the typical Saharan dust event (SI, sheet 3).

3.3. Nutrient fluxes from riverine and wet atmospheric deposition into the Annaba Bay

The DON inputs from SR and MR accounted for 10–13% of the riverine TDN input, while the fraction of DON in the WAD flux was higher, ranging from 17 to 28% (average = 23%) of TDN (Table 3). When partitioning the total TDN load into the Annaba Bay (MR + SR + AB) between riverine and WAD contributions, riverine contribution was 9-fold higher compared to the WAD. The N-NO_3 and DON loading rates for the MR catchment were higher compared to the SR, reaching 73.5 and 18.1 t N km^{-2} yr^{-1}, respectively.

The DIP flux from the WAD varied from 2.31 t P km^{-2} y^{-1}during the severe drought of 2016 to 10.5 t P km^{-2} yr^{-1} in 2014, and was on average 15.4 times lower than the riverine DIP flux (Table 3). The annual DIP loads from the SR also varied considerably, with higher loads during 2012 (97 t P km^{-2} yr^{-1}) and 2015 (73 t P km^{-2} yr^{-1}). Similarly, the DIP load in the MR increased remarkably during the years with flooding events, transporting large quantities of DIP into the Annaba Bay (Table 3).

The riverine Si loads were generally high, except for 2016 (drought year) and 2014 (relatively dry year). The Si loads from the MR were especially elevated during 2012 (2598 t Si km^{-2} yr^{-1}) and 2015 (2408 t Si km^{-2} yr^{-1}) (Table 3). In addition, the multiannual mean Si yield for the MR (470 t Si km^{-2} yr^{-1}) was more than 2-fold higher compared to the SR. Precipitation over the Annaba region deposited large amounts of Si (6.2 mmol m^{-2} yr^{-1} on average). The maximum WAD flux over the Annaba Bay was recorded during 2015 (91.4 t Si km^{-2} yr^{-1}) as a result of the rainy winter season. However, given the small surface area of the Annaba Bay (400 km^2) relative to its drainage area (10,000 km^2), the mean multiannual Si yield remained significant (174 t Si km^{-2} yr^{-1}), and comparable to that of the SR catchment (Table 3).

At a seasonal scale, a majority of the riverine and WAD nutrient inputs occurred during the rainy season. For example, the wet season contributed >82% of the annual N-NH_4 flux and 73% (2015) to 92.3% (2017) of the annual N-NO_3 fluxed (SI, sheet 2). Overall, the wet season had the controlling influence on the WAD fluxes for all nutrients and was responsible for more than 80% of the annual flux, implying that the measurements of nutrient depositions through precipitation could be limited to the wet season only.

4. Discussion

4.1. Main Algerian rivers feature compared to the Mediterranean rivers

The 2012–2017 study period encompassed the varying hydrological conditions in the Annaba region. Heavy rainfall events (late February) during 2012 and 2015 triggered large river flooding, especially in the MR catchment. In contrast, 2016 was characterized by severe drought conditions. The year 2014 was relatively dry, while 2013 and 2017 could be classified as normal years. These varying wet and drought conditions have affected both the atmospheric deposition and riverine inputs of freshwater and nutrients. Collectively, the MR and SR discharged annually an average of 1.4 km^3 of freshwater into the Annaba Bay, with a maximum of 2.28 km^3 during 2012 and a minimum of 0.59 km^3 during 2016. Approximately 60% of the discharge was carried out by the MR.

The combined discharge of the MR and SR accounts for approximately 33% the total freshwater discharge entering the Southwest Mediterranean (an average of 7 km^3 for the 1991–2000 period, Ludwig et al., 2009). The MR, with an average annual discharge of 0.88 km^3, is the largest river in Algeria (e.g., UNEP/MAP, 2013, Table 4). Although the MR has a limited catchment area and discharge period (about 5–8 months), it alone accounts for about 13% of the total riverine discharges into the Southwest Mediterranean. Although several Algerian rivers have significant freshwater discharges (e.g., Ounissi and Bouchareb, 2013; Ounissi et al., 2014), they have rarely been considered in regional studies. A comparison of various recent estimates of the Mediterranean river discharges showed a wide range of uncertainties regarding the freshwater volumes (e.g., Philandras et al., 2011; UNEP/MAP, 2013;

Table 3
Annual nutrient loading (t yr^{-1}) and yields (kg km^{-2} $yr^{-1}$and mmol m^{-2} yr^{-1}) to the Annaba region (AA) and Annaba Bay (AB) from riverine (SR and MR) and atmospheric sources during the 2012–2017 study period; the wet atmospheric deposition to AB has been converted to t yr^{-1} by multiplying the loading over AA (mmol m^{-2} yr^{-1}) by its surface area (400 km^2).

			$N\text{-}NH_4$	$N\text{-}NO_3$	$N\text{-}NO_2$	DIN	DON	TDN	DIP	Si
2012	SR	t yr^{-1}	454	506	55	1015	114	1129	97	1897
		kg km^{-2} yr^{-1}	69.8	77.8	8.5	156.2	17.5	173.7	14.9	291.8
	MR	t yr^{-1}	86	200	46	333	123	456	56	2598
		kg km^{-2} yr^{-1}	26.9	62.5	14.4	104.1	38.4	142.5	17.5	811.9
	SR + MR	t yr^{-1}	540	707	101	1347	238	1585	153	4495
		kg km^{-2} yr^{-1}	56.3	73.6	10.5	140.3	24.8	165.1	15.9	468.2
	AA	mmol m^{-2} yr^{-1}	6.9	8.8	0.6	16.3	5.3	21.5	0.4	5.9
	AB	t yr^{-1}	38.8	49.1	3.3	91.1	29.5	120.6	4.9	66.4
		kg km^{-2} yr^{-1}	97	122.8	8.3	227.8	73.8	301.5	12.3	166
	SR + MR/AB	kg:kg	13.9	14.4	30.6	14.8	8.1	13.1	31.2	67.7
2013	SR	t yr^{-1}	297	162	46	505	47	552	59	1248
		kg km^{-2} yr^{-1}	45.7	24.9	7.1	77.7	7.2	84.9	9.1	192.0
	MR	t yr^{-1}	107	209	18	334	71	405	38	1125
		kg km^{-2} yr^{-1}	33.4	65.3	5.6	104.4	22.2	126.6	11.9	351.6
	SR + MR	t yr^{-1}	404	371	64	839	118	957	96	2373
		kg km^{-2} yr^{-1}	42.1	38.6	6.7	87.4	12.3	99.7	10.0	247.2
	AA	mmol m^{-2} yr^{-1}	9.7	7.1	0.8	17.7	3.5	21.2	0.5	6.7
	AB	t yr^{-1}	54.5	39.7	4.7	98.9	19.6	118.5	6	75
		kg km^{-2} yr^{-1}	136.3	99.3	11.8	247.3	49	296.3	15	187.5
	SR + MR/AB	kg:kg	7.4	9.3	13.6	8.5	6.0	8.1	16.0	31.6
2014	SR	t yr^{-1}	121	202	40	362	47	409	34	720
		kg km^{-2} yr^{-1}	18.6	31.1	6.2	55.7	7.2	62.9	5.2	110.8
	MR	t yr^{-1}	68	316	20	404	40	444	34	921
		kg km^{-2} yr^{-1}	21.3	98.8	6.3	126.3	12.5	138.8	10.6	287.8
	SR + MR	t yr^{-1}	188	518	59	766	87	853	68	1640
		kg km^{-2} yr^{-1}	19.6	54.0	6.1	79.8	9.1	88.9	7.1	170.8
	AA	mmol m^{-2} yr^{-1}	5.7	9.4	1.1	16.2	3.4	19.7	0.9	8.1
	AB	t yr^{-1}	32.1	52.7	6	90.8	19.3	110.1	10.9	90.7
		kg km^{-2} yr^{-1}	80.3	131.8	15	227	48.3	275.3	27.3	226.8
	SR + MR/AB	kg:kg	5.9	9.8	9.8	8.4	4.5	7.7	6.2	18.1
2015	SR	t yr^{-1}	214	340	47	601	80	681	73	1627
		kg km^{-2} yr^{-1}	32.9	52.3	7.2	92.5	12.3	104.8	11.2	250.3
	MR	t yr^{-1}	65	466	40	570	39	609	75	2408
		kg km^{-2} yr^{-1}	20.3	145.6	12.5	178.1	12.2	190.3	23.4	752.5
	SR + MR	t yr^{-1}	279	806	87	1172	119	1291	148	4035
		kg km^{-2} yr^{-1}	29.1	84.0	9.1	122.1	12.4	134.5	15.4	420.3
	AA	mmol m^{-2} yr^{-1}	6.5	9.2	1.0	16.7	6.4	23.1	0.6	8.2
	AB	t yr^{-1}	36.6	51.5	5.5	93.5	35.6	129.1	7.2	91.4
		kg km^{-2} yr^{-1}	91.5	128.8	13.8	233.8	89	322.8	18	228.5
	SR + MR/AB	kg:kg	7.6	15.7	15.8	12.5	3.3	10.0	20.6	44.1
2016	SR	t yr^{-1}	139	148	32	319	27	347	17	616
		kg km^{-2} yr^{-1}	21.4	22.8	4.9	49.1	4.2	53.4	2.6	94.8
	MR	t yr^{-1}	62	115	38	215	26	241	10	223
		kg km^{-2} yr^{-1}	19.4	35.9	11.9	67.2	8.1	75.3	3.1	69.7
	SR + MR	t yr^{-1}	201	263	70	535	53	588	27	839
		kg km^{-2} yr^{-1}	20.9	27.4	7.3	55.7	5.5	61.3	2.8	87.4
	AA	mmol m^{-2} yr^{-1}	4.7	6.8	0.6	12.1	4.4	16.5	0.2	3.8
	AB	t yr^{-1}	26.2	37.9	3.5	67.7	24.5	92.1	2.3	42.9
		kg km^{-2} yr^{-1}	65.5	94.8	8.8	169.3	61.3	230.3	5.8	107.3
	SR + MR/AB	kg:kg	7.7	6.9	20.0	7.9	2.2	6.4	11.7	19.6
2017	SR	t yr^{-1}	565	109	55	729	88	817	35	1324
		kg km^{-2} yr^{-1}	86.9	16.8	8.5	112.2	13.5	125.7	5.4	203.7
	MR	t yr^{-1}	230	105	44	379	49	429	26	1756
		kg km^{-2} yr^{-1}	71.9	32.8	13.8	118.4	15.3	134.1	8.1	548.8
	SR + MR	t yr^{-1}	795	215	99	1108	137	1246	61	3080
		kg km^{-2} yr^{-1}	82.8	22.4	10.3	115.4	14.3	129.8	6.4	320.8
	AA	mmol m^{-2} yr^{-1}	9.5	8.0	0.8	18.3	5.7	24.0	0.7	4.6
	AB	t yr^{-1}	53.4	44.9	4.2	102.4	31.9	134.3	9	51.3
		kg km^{-2} yr^{-1}	133.5	112.3	10.5	256	79.8	335.8	22.5	128.3
	SR + MR/AB	kg:kg	14.9	4.8	23.6	10.8	4.3	9.3	6.8	60.0

Wang and Polcher, 2019). Wang and Polcher (2019) suggested that discharges from many ungauged coastal rivers are not taken into account, which contributes to the uncertainty in the regional freshwater budgets.

During the 2012–2017 study period, the MR consistently have higher nutrient loads compared to the SR. The only exception was $N\text{-}NH_4$ loading, which was higher for the SR, reaching a maximum rate of 543 kg N km^{-2} yr^{-1} in 2009 (SI, sheet 4). The NH_4 contributed between 42 and 82% of the TDN load in the SR. This stands in sharp contrast to most other Mediterranean rivers where, as a result of fertilizer application in the watersheds, the NO_3 fraction is typically the major contributor to the TDN (Garnier et al., 2010; Malagó et al., 2019).

For example, the $N\text{-}NO_3$ yields for the Po and Rhone Rivers are 40-fold and 22-fold higher, respectively, compared to the $N\text{-}NO_3$ yields for the SR. Overall, a majority of the Mediterranean rivers have elevated NO_3 and DIN levels and yields compared to the Algerian rivers (SI, sheet 4). The strong dominance of NH_4 in SR waters is predominantly a consequence of the direct wastewater inputs originating from domestic

Table 4
A comparison of atmospheric and riverine nutrient inputs (mmol m^{-2} yr^{-1}) for selected Mediterranean regions and world seas.

Site	NH_4	NO_3	DIN	DIP	DSi	Reference[f]
SW Mediterranean						
Atmospheric[g]	7.2	8.2	16.2	0.54	6.2	This study
Riverine			17.3	0.66	9.48	Ludwig et al. (2009)
W Mediterranean						
Atmospheric			38.3	0.54	0–6.7[a]	Guerzoni and Molinaroli (2005)
Riverine			26.2	1.17	19.64	Ludwig et al. (2009)
North Levantine Sea						
Atmospheric	38	125	163	0.69	1.43	Koçak et al. (2010)
Riverine			28.6	1.1	20.1	Ludwig et al. (2009)
E Mediterranean						
Atmospheric	24	40	64	0.81	0.74[b]	Herut et al. (1999, 2002)
Riverine			7.12	0.27	4.8	Ludwig et al. (2009)
Mediterranean						
Atmospheric			31.97	0.9	2.93[c]	Guerzoni et al. (1999)
Riverine			28.75	1.88	6.6[d]	Guerzoni et al. (1999)
Black Sea						
Atmospheric	31.9	17.5	49.4	3.13		Medinets and Medinets (2012)
Riverine			37.3	0.96	13.0	Ludwig et al. (2009)
Baltic Sea						
Atmospheric	18.9	20.8	39.7	0.18		Rolff et al. (2008)
Riverine			27.6	0.64		Mörth et al. (2007)
North Sea						
Atmospheric			39			Rendell et al. (1993)
Riverine			100			Rendell et al. (1993)
East China Sea						
Atmospheric			105	0.32	3.4	Song (2011)
Riverine			125[e]	0.27	45.7	Song (2011)
Southern Yellow Sea						
Atmospheric	23.8	28.1	52	0.72	2.6	Song (2011)
Riverine	7.7	48.7	57	0.59	173	Song (2011)
Southern California Bight						
Atmospheric	16	25	41			Howard et al. (2014)
Riverine	6	32	38			Howard et al. (2014)
Northeast United States						
Atmospheric		85.7				Howarth et al. (2002)
Riverine		56.4				Howarth et al. (2002)
Sea of Japan						
Atmospheric	34	43	77			Sugimoto and Tsuboi (2017)
Riverine			140			Sugimoto and Tsuboi (2017)

[a] Treguer et al. (1995)
[b] Krom et al. (2014).
[c] Mean of the different listed Mediterranean regions.
[d] Ludwig et al. (2009) and all values DIN and DIP are total N and total P respectively from riverine inputs for this reference.
[e] Tong et al. (2015).
[f] Note that simultaneaous atmoshpheric and riverine measurements (estimations) are those that reffer to the same author; in the other cases, comparisons between riverine and atmopheric inputs might be somehow difficult.
[g] Wet deposition.

and urban sources along the lower catchment. Although the NH_4 levels in the SR waters decreased by 4-fold during the last decade (owing to the improvement of wastewater treatment), the SR remains one of the most polluted river in the Mediterranean region (SI, sheet 4). For example, the SR has one of the highest N-NH_4 yield among the Mediterranean coastal rivers, along with selected Turkish, Greek (Pinios, Evros) and Italian (Po, Reno) rivers (SI, sheet 4). Nevertheless, the SR ad MR have significantly lower DIN yields compared to other Mediterranean rivers, i.e., 2.5-fold lower than the DIN yields for the Southwestern Mediterranean rivers (SI, sheet 4). Importantly, the MR has the lowest reported NO_3 levels and yields among the Mediterranean rivers, with the N-NO_3 multiyear mean yield 22 and 12 times lower compared to the Po and Rhone Rivers, respectively. The low NO_3 levels in the MR reflect both the sparse agricultural activities in the MR watershed (4–5% of irrigated area, UNEP/MAP, 2013) and also the nutrient retention in multiple water bodies (reservoirs, marchlands, estuary) within the MR watershed. The MR waters are so impoverished in all TDN species that could sensibly be compared to the rainwater. Interestingly, the average of NH_4 levels in rainwater are 1.5-fold higher compared to the MR. Similarly, the DON concentrations and yields in the MR were among the lowest reported for the Mediterranean rivers (Table 4, UNEP/MAP, 2013). These features make the MR a singular riverine ecosystem in the Mediterranean region.

The DIP loads from the SR were exceptionally high during the flood years (e.g., 2012 and 2015) when the DIP yield increased to 12–15 kg P km^{-2} yr^{-1}. The maximum DIP yield for both the SR and MR (40.5 and 28 kg P km^{-2} yr^{-1}, respectively) was also recorded during the wet year of 2009 (SI, sheet 4). As shown in SI, sheet 4, most of the North Algerian coastal rivers have high DIP and N-NH_4 yields, which are indicative of domestic and urban wastewater contamination. This contrasts sharply with most other Mediterranean rivers, which generally displayed a reduction in DIP over time and constant but high N-NO_3 deliveries (Moon et al., 2016).

The worsening water quality in the SR is evidenced from the imbalanced stoichiometric N:P ratios. Most of the elevated N:P ratios occurred during high river discharge, while low values occurred during dry periods when DIP was delivered in excess over DIN. The MR also displayed imbalanced N:P ratios, mostly during the outlet closing period (N:P < 10, about 38% of cases) or under high river discharge regimes (N:P > 20, in about 42% of cases). During the outlet closing period, the MR is isolated from both continental and marine influence for several months, and thus the receiving coastal waters do not experience the deteriorated water quality during that time. Despite a departure from the Redfield ratio, the N:P ratios for both the MR and SR waters remain much lower compared to the other Mediterranean rivers (SI, sheet 4). Cozzi et al. (2018) also reported that all large rivers flowing into the Mediterranean experience heavy disturbances in the N:P molar ratios, where N:P ratios >50 are becoming increasingly common.

When compared to the average DSi value for the Mediterranean rivers (140 μmol L^{-1}, Ludwig et al., 2009; Dürr et al., 2011; Romeo et al., 2013), the SR and MR can be characterized as deficient in Si. As is the case with the TDN and DIP, the low DSi concentrations in the MR are related to the Si removal in the reservoirs upstream and the influence of cascading filters (lateral wetlands, shallow lentic waters and estuarine reaches) that impede the MR flow. Viaroli et al. (2015) reported that the cascading filters in the Po River watershed (North Adriatic) influence the downstream nutrient availability, stoichiometry and water quality. The reported Si yields for various Mediterranean rivers varied over a wide range, from 134 kg Si km^{-2} yr^{-1} in the Eastern Mediterranean to 799 kg Si km^{-2} yr^{-1} in the Northwestern Mediterranean. The mean Si yield for the MR averaged 379 kg Si km^{-2} yr^{-1} during the 2012–2017 study period. This value is much lower compared to global averages (e.g., 1400 kg Si km^{-2} yr^{-1}, Dürr et al., 2011). The DSi multiyear mean concentration and yield for the SR were about one-half and one-third, respectively, of the values reported for the European and Mediterranean rivers (Dürr et al., 2011; Romero et al., 2013). In addition to estuarine buffering (Jickells et al., 2014; Viaroli et al., 2015), the retention behind dams is likely responsible for the pronounced decline in the DSi levels, as has been reported for several Algerian rivers (Ounissi and Bouchareb, 2013).

The low DSi concentrations in the SR, in conjunction with the elevated DIN levels, have resulted in very low and largely imbalanced stoichiometric ratios (Si:N = 0.84), with about 70% of samples displaying Si:N ratios below 1. On the other hand, because the Si:N ratios <1 generally coincided with the low river discharges, the effects of altered nutrient ratios on the receiving coastal waters are not clear. At

regional and global scales, the imbalanced Si:N ratios have become increasingly common in European rivers (e.g. Romero et al., 2013), Mediterranean rivers (Romero et al., 2013; Powley et al., 2017; Cozzi et al., 2018) and many rivers worldwide (e.g., Garnier et al., 2010). Based on the Si:N:P ratios and fluxes, Billen and Garnier (2007) proposed an indicator of coastal eutrophication potential (ICEP) to assess the potential of river systems for coastal eutrophication, whereby the excess in N and P over Si results in the new production of non-siliceous algae. Using this approach, Garnier et al. (2010) and Romero et al. (2013) concluded that an excesses in N and P over Si in most Mediterranean and North Atlantic rivers point to a potential risk of eutrophication in the receiving coastal waters.

Contrary to the SR, the MR had a more balanced Si:N ratios (Si:N = 2.2), except during the outlet closing period. In the case of MR, the cascading filters have likely reduced both the N and Si levels and thus modulated the stoichiometry of those nutrients. Moreover, most of the potential risk of eutrophication (excess of N or P over silica) is associated with the dry periods, which is also when the coastal waters of Annaba Bay are most stratified (Ounissi et al., 2016). This synergistic influence could enhance eutrophication risks (Frehi et al., 2007), particularly during transitional periods (May and September–October) when storm events can trigger large river discharges. Importantly, harmful dinoflagellates bloom are becoming increasing common in the innermost section of the Annaba Bay (Frehi et al., 2007; Ounissi et al., 2016). These outbreaks of eutrophication are fueled by the increased loading of dissolved nutrients from the SR and MR. Another contributing factor is a significant loading of particulate matter, as high as 102 kt yr^{-1}, that is rich in both organic carbon (4.5%) and biogenic silica (1%, Ounissi et al., 2018).

4.2. *Atmospheric nutrient input features over Annaba Bay and comparison with Mediterranean regions*

In addition to the riverine nutrient loading, the Annaba Bay also received significant amounts of nutrients from the wet atmospheric deposition (WAD). The WAD fluxes of DIN and DON for the Annaba region are among the lowest for the Mediterranean coastal areas (SI, sheet 5). The only exception is the Gulf of Gabes, Tunisia, which has even lower WAD values, comparable to the natural background levels in the southern ocean (e.g., Guerzoni and Molinaroli, 2005). Relatively low DIN (16.2 mmol N m^{-2} yr^{-1}) and DON (4.77 mmol N m^{-2} yr^{-1}) depositions over the Annaba region are related to the low anthropogenic emission from the agriculture, industry and traffic across the region. For a densely populated area of Guangzhou, China, (13.3×10^6 people), Li et al. (2012) reported an exceptionally high levels and yields of DON, averaging 35 μmol L^{-1} and 58.9 mmol N m^{-2} yr^{-1}, respectively. This DON flux is 3.7 times higher than the world average (15.7 mmol N m^{-2} yr^{-1}) reported in the review of Neff et al. (2002). Similarly, Zhang et al. (2012) reported strong high DON levels (mean = 77 μ μmol L^{-1}) and yields (mean = 49 mmol N m^{-2} yr^{-1}) across 32 sites throughout China. However, for the global ocean, Kanakidou et al. (2012) reported that DON is mainly deposited with rain events (60.2%), from which 61% is of anthropogenic origin. Similarly, about 50% of TDN atmospheric deposition flux is from terrestrial anthropogenic activities (Kanakidou et al., 2018).

On the other hand, the DON input from WAD over the Annaba region mostly occurred during the wet season (82.7%) and represented 23% the TDN yield. This is in agreement with both the fraction within TDN (31.6%) and yield (4.8 mmol N m^{-2} yr^{-1}) reported by Violaki et al. (2010) for 12 coastal areas around the Mediterranean Sea. The latter study also estimated that between 20 and 30% of the new production in the Eastern Mediterranean could be sustained by the atmospheric DON deposition. Also, Guerzoni and Molinaroli (2005) estimated that the atmospheric N deposition over the oligotrophic open waters of the Mediterranean, may account for up to 60% of the new production.

In contrast to the TDN, the atmospheric inputs of DIP and Si recorded for the Annaba area are the highest among the 20 Mediterranean coastal sites (SI, sheet 5). These high deposition rates could be related to the Saharan dust transport from the adjacent Algerian desert. Guerzoni and Molinaroli (2005) reported a high dust loading over the southern Sardinia (6–13 g m^{-2} yr^{-1}), which is located 225 km to the north from the Annaba. Moreover, Guerzoni et al. (1992) also demonstrated that in 75% of the cases deposition of the Saharan dust over Sardinia was associated with rainfall events. Also, for Corsica, located further to the north from Sardinia, Desboeuf et al. (2018) reported an exceptionally high WAD of Si (7.3 mmol Si m^{-2} yr^{-1}, as bulk deposition), of which 57% was related to the high dust load events. This study further estimated that the WAD was responsible for 84% the total atmospheric Si deposition. This value is comparable to that of the Annaba region, and is among the highest measured for the Mediterranean. This implies that our study area, which is adjacent to the Algerian Saharan region, could receive more mineral dust compared to the more distant Northwestern Mediterranean regions. In fact, for the southern Spain (Sierra Nevada) region, which is also influenced by dust intrusion from North Africa, Morales-Baquero et al. (2013) reported a rather low Si WAD value (0.80 mmol Si m^{-2} yr^{-1}). Similarly, in the Northeastern Mediterranean (Erdemli, Turkey), Si levels increased by at least 33% during sporadic dust events from both the North African and Middle Eastern origins (Koçak et al., 2010). Nevertheless, it is important to highlight the significant lack of data on atmospheric Si deposition for the Mediterranean as a whole (see available data in SI, sheet 5), which, given the heterogeneity of sampling methods (wet, dry, bulk, total depositions), make any comparison difficult. The DIP deposition data for the Mediterranean have a larger coverage, although some notable gaps still exist, as can be seen from SI, sheet 5.

As shown in SI, sheet 5, the highest DIP deposition rate for the entire Mediterranean region was measured in North Africa (Cap Spartel, Morocco, Markaki et al., 2010), although it should be pointed out that this particular value concerns the bulk deposition. The high DIP deposition rates (> 0.5 mmol P m^{-2} yr^{-1}) are typically encountered in the Western Mediterranean, and probably reflect the differences in precipitation among the Western and the Eastern Mediterranean regions. Markaki et al. (2010) observed a similar pattern with higher deposition rates over the Western Mediterranean (0.55 mmol P m^{-2} yr^{-1}) and relatively low values over the Eastern Mediterranean regions (0.38 mmol P m^{-2} yr^{-1}). Regardless of the regional differences, the atmospheric DIP deposition rates for the Mediterranean are generally high and may account for up to 25% of new production in the Mediterranean oligotrophic regions (Guerzoni and Molinaroli, 2005).

Overall, the low WAD rates of TDN over the Annaba region, associated with relatively higher DIP and Si depositions, have resulted in lower N:P and higher Si:N molar ratios in comparison with other Mediterranean regions. Moreover, Christodoulaki et al. (2016) suggested that atmospheric deposition alone could explain the unusually high N:P ratio observed in the Mediterranean waters. At the seasonal scale, there is a substantial decrease in N:P ratio during the dry season (average = 47.5), presumably due to the increase in DIP deposition relative to DIN. The controlling influence of the Saharan airflow during the dry season can supply significant amounts of DIP and thus modify the nutrients levels and stoichiometry. The pH of pure Saharan rain over Corsica was estimated to be >6.8 and the rainfall events with pH > 6 could be affected by Saharan dust in 68% of cases (Loÿe-Pilot et al., 1986). Also, in Corsica, the pH of the rainfall influenced by the Saharan dust events varied between 6.5 and 7.97 (Guieu et al., 2002). In our study area, for example, among 117 rainwater samples, 84% had pH values >6 (SI, sheet 3). An average pH value of 7.0 was typical for the dry season. This suggests that about 84% of the precipitation events occurring over the Annaba region could be of Saharan origin. In fact, it has been recognized that the Saharan dust transport episodes over the Western Mediterranean regions have become more frequent, and constitute an important source of nutrients (Escudero et al., 2005; Morales-Baquero et al., 2013; Castillo et al., 2017).

On the other hand, given the relatively high DSi and low DIN levels in the precipitation over the Annaba region that were recorded during our 2012–2017 study, the Si:N molar ratios are elevated (0.38–0.78) and comparable to the Si:N ratios of the Mediterranean rivers. Also, for the same reason, a comparable Si:N value (0.60) was observed in the Gulf of Gabes, Tunisia (Khammeri et al., 2018). The average Si:N ratio for the entire Mediterranean region could be as low as 0.05 (SI, sheet 5). This excess of N over DSi in atmospheric deposition, combined with similar alterations in nutrients stoichiometry of the Mediterranean rivers (Garnier et al., 2010; Romero et al., 2013), could further increase the potential for eutrophication across the Mediterranean coastal waters.

4.3. Atmospheric versus riverine nutrient inputs and comparison with main world seas

The Annaba Bay annually received on average 1052 t of DIN and 152 t of DON, from which the WAD accounted for 17.6% of DON and only 8.6% of DIN. The WAD contributions of N-NH_4 and N-NO_3 are only about of 9%. Likewise, most of the annual DIP and Si loads entering the Annaba Bay are of riverine origin. In particular, the WAD contribution to the total Si and DIP loads are about 2.5% and 7%, respectively. This suggests that the Annaba Bay, because of the high drainage area/bay area ratio, has much stronger riverine influence compared to other Mediterranean bays. In many other marginal seas with large drainage/surface area ratio and high precipitation (North Sea, Sea of Japan, East China Sea, Yellow Sea), the riverine inputs of DIN and Si have been reported to be higher than the atmospheric deposition (Table 4). As has been suggested before (Milliman, 2001), land-ocean interface may not be limited to the river mouth, but might holistically include the river watersheds that drain into coastal waters. However, most of the Mediterranean coastal regions have limited drainage areas and precipitation yields, and are additionally affected by significant water retention behind the dams (e.g., Ludwig et al., 2009). In the extreme cases, this could lead to the dominance of atmospheric nutrient inputs over the riverine ones. For example, in the North Levantine basin (Erdemli, NE Mediterranean Sea), the DIN and DIP loads are mostly provided by the WAD, contributing 90% and 60%, respectively, the total DIN and DIP inputs (Koçak et al., 2010). Similarly, the recent work of Powley et al. (2017) found a large excess in the atmospheric DIN and DIP deposition over riverine DIN and DIP inputs for both the Western and the Eastern Mediterranean regions.

The atmospheric nutrient inputs over the Annaba Bay are characterized by the low DIN deposition and high DIP and Si depositions and more balanced stoichiometric ratios compared to other Mediterranean regions. This is likely to have important biogeochemical implications for the bay ecosystem, which has otherwise been characterized as an oligotrophic region from its entrance (about 12 km from the MR and SR outlets) to the outer open region (Frehi et al., 2007).

The significance of atmospheric nutrient deposition can be illustrated by calculating the potential for new primary production that can be generated by the atmospheric deposition of nutrients. If the WAD nutrient values over the Annaba Bay (see Table 3) are converted into the equivalent primary production rates using the Redfield stoichiometry (C:N:P:Si = 106:16:1:1), and assuming that all the wet-deposited DIP is used by phytoplankton, the estimated new production values range from 1.13 to 2.96 g C m^{-2} yr^{-1}. For DIN depositions, the equivalent potential carbon production rates range from 1.12 to 1.73 g C m^{-2} yr^{-1}. Also, the new phytoplankton production (as diatoms) sustained by DSi depositions would be between 0.7 and 1.5 g C m^{-2} yr^{-1}. Similarly, the potential new production that could be sustained by the riverine nutrient inputs (see Table 3) can also be estimated. The riverine DIP, DIN and DSi loads can sustain a new production of 24.3, 15.9 and 44.8 g C m^{-2} yr^{-1}, respectively. When combined, the riverine and atmospheric nutrient inputs could support the new primary production rates for the Annaba Bay of 26, 17.4 and 46 g C m^{-2} yr^{-1} from DIP, DIN and DSi contributions, respectively. However, other external nutrient sources, such as the point sources and groundwater discharges, also contribute to the primary production. However, because the stoichiometry of both riverine and atmospheric nutrient suggests that primary production in the Annaba Bay is co-limited by Si and P, the potential new production would more strongly respond to the delivery of those nutrients, particular during the dry season where the nutrients stoichiometric ratios are usually unbalanced. Both the P—Si co-limitation (Powley et al., 2017) and the Si-limitation (Garnier et al., 2010; Romero et al., 2013; Cozzi et al., 2018) are well documented for the Western Mediterranean regions. On the other hand, when compared to the primary production rates reported for the Western Mediterranean (around 150–160 g C m^{-2} yr^{-1}: Bosc et al., 2004; Lazzari et al., 2012; Powley et al., 2017), the potential new production is on the order of 12%. This value is comparable to the estimate reported by Lazzari et al. (2012) for the Ionian Sea (16%), but much lower than that of Béthoux (1989) for the Western Mediterranean (36%). Evidently, regional differences in primary production estimates reflect the differences in both riverine and atmospheric nutrient inputs.

5. Conclusions

This study describes the first contemporaneous long-term effort to examine the nutrient inputs to the southern Mediterranean Sea from rivers and wet atmospheric deposition. During the 6-year study period (2012–2017) the Annaba region has experienced highly variable hydrological conditions that ranged from heavy rainfall and river flooding during 2012 and 2015 to severe drought conditions during 2016. Collectively, the MR and SR discharged annually into the Annaba Bay 2.28 km^3 during 2012, which represents approximately 33% the total river discharges entering the Southwestern Mediterranean. With an annual average discharge of about 0.90 km^3 the MR can be considered the most important river in Algeria. Consequently, the MR yielded more nutrients than the SR, except for N-NH_4.

Although NH_4 levels in the SR waters decreased by 4-fold during the last decade (owing to the improvement of wastewater treatment), the SR remains heavily polluted, with the highest N-NH_4 and DIP yields among the Mediterranean coastal rivers. Most of the Algerian coastal rivers exhibited both strong DIP and N-NH_4 yields, and seem to be suffering from domestic and urban waste pollution.

Nevertheless, the DIN and N-NO_3 yields for both the SR ad MR were the lowest compared to the reported values for different Mediterranean rivers. The reduced NH_4, NO_3, and DON levels not only reflect the subtle human influence on the MR watershed but also the role of cascading filters (reservoirs, marchlands, floodplain, and estuary) that play an important role in controlling the nutrient inflow to the sea. The MR waters were so impoverished in all TDN fractions that could sensibly be compared to the rainwater. These features make the MR a unique ecosystem in the Mediterranean region.

DIP yields in the SR and MR catchments appeared to be small when compared to the other Mediterranean rivers, decreasing to only 2–3 kg P km^{-2} yr^{-1} during the drought years.

The SR water quality worsening is also evident from the imbalanced stoichiometric Si:N:P ratios, with most of the elevated N:P ratios occurring during the high river discharges. The MR showed unbalanced nutrient ratios values mostly during the outlet closing period, and thus the water quality of the receiving coastal waters was not adversely affected.

The SR and MR can be characterized as depleted in DSi compared to other Mediterranean coastal rivers. The DSi yield for the SR is about one-third the average for the European and Mediterranean rivers. In the SR, the low DSi levels are associated with the high DIN levels, resulting in low and imbalanced stoichiometric Si:N ratios (< 1). The decrease in the MR DSi levels can be related to the DSi removal within the upstream reservoirs and other cascading filters. However, the MR is characterized by higher and more balanced Si:N ratios, except during the outlet closing period when the river did not reach the Annaba Bay. The alteration of

nutrients stoichiometry (excess of DIN and DIP over DSi) in the SR and MR could increase the potential of eutrophication risk across the Annaba coastal region.

The WAD fluxes of DIN and DON deposition rates over the Annaba region are among the lowest in the Mediterranean coastal areas, owing to the low anthropogenic emission across the area. The DON inputs from precipitation mostly occurred during the wet season (82.7%) and represented 23% the TDN yield. In contrast, the atmospheric inputs of DIP and DSi over the study area were the highest in the Mediterranean region, with about 80% of the annual atmospheric depositions occurring during the wet season. These high deposition rates are associated with the Saharan dust inputs from the contiguous Algerian desert. About 84% of the precipitation events occurring over the Annaba region could be of Saharan origin, as 84% of rainwater samples exhibited typical Saharan pH values (> 6).

The low TDN and the high DIP and DSi values in the WAD over the Annaba Region resulted in relatively low stoichiometric N:P ratios and high Si:N ratios. These elevated Si:N ratios in rainwater are comparable to those of the Mediterranean rivers.

The atmospheric deposition of nutrients contributed less than 9% of the total nutrient load entering the Annaba Bay, except for DON which accounted for 17.6% the riverine inputs. This suggests that the Annaba Bay is more continental-influenced compared to other Mediterranean coastal bays, primarily because of the high drainage area/bay area ratio.

The main characteristics of the atmospheric nutrient inputs over the Annaba Region are the low DIN deposition, high DIP and Si depositions, and more balanced stoichiometric nutrient ratios compared to other Mediterranean coastal regions. This could have important biogeochemical consequences for the oligotrophic open waters of Annaba Bay, given that the potential new production that could be triggered by atmospheric and riverine DIN inputs is $\sim$19 g C m^{-2} yr^{-1}. However, the stoichiometry of both riverine and atmospheric nutrient inputs is strongly indicative that primary production in the receiving waters is co-limited by Si and P. As the roles of the anthropogenic and natural nutrient enrichment are becoming critical in the context of global climate change, a more complete assessment of the contemporaneous atmospheric and riverine nutrient inputs to the Mediterranean Sea is urgently needed.

Declaration of Competing Interest

None.

Acknowledgments

This research was supported by CNEPRU project D00L03UN230120120003, funded by the Algerian Minister of Higher Education and Scientific Research. It contributes to ChArMEx WP5 on atmospheric deposition and to MerMex studies on biogeochemical responses to nutrient forcing. The authors would like to thank the Editor and two anonymous reviewers for their valuable comments to improve the manuscript.

Appendix A. Supplementary data

Supplementary data to this article can be found online at https://doi.org/10.1016/j.marchem.2020.103915.

References

Barkley, A.E., Prospero, J.M., Mahowald, N., Hamilton, D.S., et al., 2019. African biomass burning is a substantial source of phosphorus deposition to the Amazon, Tropical Atlantic Ocean, and Southern Ocean. PNAS. https://doi.org/10.1073/pnas.1906091116.

Bergametti, G., Remoudaki, E., Losno, R., Steiner, E., Chatenet, B., Buat-Menard, P., 1992. Source, transport and deposition of atmospheric phosphorus over the northwestern Mediterranean. J. Atmos. Chem. 14 (1–4), 501–513. https://doi.org/10.1007/BF00115254.

Béthoux, J.P., 1989. Oxygen consumption, new production, vertical advection and environmental evolution in the Mediterranean Sea. Deep-Sea Res. 36, 769–781.

Billen, G., Garnier, J., 2007. River basin nutrient delivery to the coastal sea: Assessing its potential to sustain new production of non-siliceous algae. Mar. Chem. 106 (1–2), 148–160. https://doi.org/10.1016/j.marchem.2006.12.017.

Bonnet, S., Guieu, C., Chiaverini, J., Ras, J., Stock, A., 2005. Effect of atmospheric nutrients on the autotrophic communities in a low nutrient, low chlorophyll system. Limnol. Oceanogr. 50, 1810–1819.

Bosc, E., Bricaud, A., Antoine, D., 2004. Seasonal and interannual variability in algal biomass and primary production in the Mediterranean Sea, as derived from 4 years of SeaWiFS observations. Global Biogeochem. Cycles 18, GB1005. https://doi.org/10.1029/2003GB00203.

Cape, J.N., Tang, Y.S., Gonzalez-Benıtez, J.M., Mitosinkova, M., Makkonen, U., Jocher, M., Stolk, A., 2012. Organic nitrogen in precipitation across Europe. Biogeosciences 9, 4401–4409. https://doi.org/10.5194/bg-9-4401-2012.

Castillo, S., Alastuey, A., Cuevas, E., Querol, X., Avila, A., 2017. Quantifying dry and wet deposition fluxes in two regions of contrasting African Influence: The NE Iberian Peninsula and the Canary Islands. Atmosphere 8, 86. https://doi.org/10.3390/atmos8050086.

Christodoulaki, S., Petihakis, G., Kanakidou, M., Mihalopoulos, N., Tsiaras, K., Triantafyllou, G., 2013. Atmospheric deposition in the Eastern Mediterranean. A driving force for ecosystem dynamics. J. Mar. Syst. 109-110, 78–93. https://doi.org/10.1016/j.jmarsys.2012.07.007.

Christodoulaki, S., Petihakis, G., Mihalopoulos, N., Tsiaras, K., Triantafyllou, G., Kanakidou, M., 2016. Human-driven atmospheric deposition of N and P controls on the east Mediterranean marine ecosystem. J. Atmos. Sci. 73, 1611–1619. https://doi.org/10.1175/JAS-D-15-0241.1.

Cloern, J.E., 2001. Our evolving conceptual model of the coastal eutrophication problem. Mar. Ecol. Prog. Ser. 210, 223–253. https://doi.org/10.3354/meps210223.

Conley, D.J., Stålnacke, P., Pitkänen, H., Wilander, A., 2000. The transport and retention of dissolved silicate by rivers in Sweden and Finland. Limnol. Oceanogr. 45 (8), 1850–1853. https://doi.org/10.4319/lo.2000.45.8.1850.

Cornell, S.E., 2011. Atmospheric nitrogen deposition: Revisiting the question of the importance of the organic component. Environ. Pollut. 159, 2214–2222. https://doi.org/10.1016/j.envpol.2010.11.014.

Cozzi, S., Ibáñez, C., Lazar, L., Raimbault, P., Giani, M., 2018. Flow regime and nutrient-loading trends from the largest south European watersheds: Implications for the productivity of Mediterranean and Black Sea's coastal areas. Water 11 (1), 1–27. https://doi.org/10.3390/w11010001.

Desboeufs, K., Nguyen, K.B., Chevaillier, S., Triquet, S., Dulac, F., 2018. Fluxes and sources of nutrient and trace metal atmospheric deposition in the northwestern Mediterranean.Atmos. Chem. Phys. 18, 14477–14492. https://doi.org/10.5194/acp-18-14477-2018.

Djaoudi, K., Van Wambeke, F., Barani, A., Hélias-Nunige, S., Sempéré, R., Pulido-Villena, E., 2018. Atmospheric fluxes of soluble organic C, N, and P to the Mediterranean Sea: Potential biogeochemical implications in the surface layer. Prog. Oceanogr. https://doi.org/10.1016/j.pocean.2017.07.008.

Duce, R.A., LaRoche, J., Altieri, K., Arrigo, K.R., Baker, A.R., et al., 2008. Impacts of atmospheric anthropogenic nitrogen on the open ocean. Science 320 (80), 893–897. https://doi.org/10.1126/science.1150369.

Dürr, H.H., Meybeck, M., Hartmann, J., Laruelle, G.G., Roubeix, V., 2011. Global spatial distribution of natural riverine silica inputs to the coastal zone. Biogeosciences 8 (3), 597–620. https://doi.org/10.5194/bgd-6-1345-2009.

Escudero, M., Castillo, S., Querol, X., Avila, A., Alarcón, M., et al., 2005. Wet and dry African dust episodes over eastern Spain. J. Geophys. Res. 110, 1–15, 1029/2004JD004731.

Frehi, H., Couté, A., Mascarell, G., Perrette-Gallet, C., Ayada, M., Kara, M.H., 2007. Dinoflagellés toxiques et/ou responsables de blooms dans la baie d'Annaba (Algérie). CR Biologie 330, 615–628. https://doi.org/10.1016/j.crvi.2007.05.002.

Friedl, G., Wüest, A., 2002. Disrupting biogeochemical cycles-Consequences of damming. Aquat. Sci. 64 (1), 55–65.

Galloway, J.N., Townsend, A.R., Erisman, J.W., Bekunda, M., Cai, Z.C., Freney, J.R., Martinelli, L.A., Seitzinger, S.P., Sutton, M.A., 2008. Transformation of the nitrogen cycle: Recent trends, questions, and potential solutions. Science 320, 889–892.

Garnier, J., Beusen, A., Thieu, V., Billen, G., Bouwman, L., 2010. N:P:Si nutrient export ratios and ecological consequences in coastal seas evaluated by the ICEP approach. Glob. Biogeochem. Cycles 24 (4). https://doi.org/10.1029/2009gb003583.

Gaume, E., Borga, M., Llasat, M.C., Maouche, S., Lang, M., Diakakis, M., 2016. Mediterranean extreme floods and flash floods. In: Hydro-meteorological extremes, chapter 3, The Mediterranean Region under Climate Change, A Scientific Update. IRD Editions, pp. 133–144.

Guerzoni, S., Molinaroli, E., 2005. Inputs of various chemicals transported by Saharan dust and depositing at the sea surface in the Mediterranean Sea. In: Saliot, A. (Ed.), The Mediterranean Sea. The Handbook of Environmental Chemistry. Springer, Germany, NJ, pp. 237–268.

Guerzoni, S., Landuzzi, W., Lenaz, R., Quarantotto, G., Cesari, G., Rampazzo, R., Molinaroli, E., 1992. Mineral atmospheric particulate from south to northwest Mediterranean: Seasonal variations and characteristics. Water Polluti. Res. Rep. 28, 483–493.

Guerzoni, S., Chester, R., Dulac, F., Herut, B., Loÿe-Pilot, M.D., Measures, C., Migon, C., Molinaroli, E., Moulin, C., Rossini, P., Saydam, C., Soudine, A., Ziveri, P., 1999. The role of atmospheric deposition in the biogeochemistry of the Mediterranean Sea. Prog. Oceanogr. 44, 147–190. https://doi.org/10.1016/S0079-6611(99)00024-5.

Guieu, C., Bonnet, S., Wagener, T., Loye-Pilot, M.D., 2005. Biomass burning as a source of dissolved iron to the open ocean? Geophys. Res. Lett. 32 (19) https://doi.org/10.1029/2005GL022962.
Guieu, C., Loÿe-Pilot, M.-D, Ridame, C., 2002. Chemical characterization of the Saharan dust end-member; some biologicalimplications for the western Mediterranean. J. Geophys. Res. 107 (D15), 4258. https://doi.org/10.1029/2001JD000582.
Herut, B., Krom, M.D., Pan, G., Mortimer, R., 1999. Atmospheric input of nitrogen and phosphorus to the Southeast Mediterranean: Sources, fluxes, and possible impact. Limnol. Oceanogr. 44 (7), 1683–1692. https://doi.org/10.4319/lo.1999.44.7.1683.
Herut, B., Collier, R., Krom, M.D., 2002. The role of dust in supplying nitrogen and phosphorus to the Southeast Mediterranean. Limnol. Oceanogr. 47 (3), 870–878. https://doi.org/10.1021/es020516d.
Howarth, R.W., Sharpley, A., Walker, D., 2002. Sources of nutrient pollution to coastal waters in the United States: implications for achieving coastal water quality goals. Estuaries 25 (4), 656–676. https://doi.org/10.1007/BF02804898.
Humborg, C., Conley, D.J., Rahm, L., Wulff, F., Cociasu, A., Ittekkot, V., 2000. Silicon retention in river basins: Far-reaching effects on biogeochemistry and aquatic food webs in coastal marine environments. Ambio J. Human Environ. 29 (1), 45–50. https://doi.org/10.1579/0044-7447-29.1.45.
Jickells, T.D., Andrews, J.E., Parkes, D.J., Suratman, S., Aziz, A.A., Hee, Y.Y., 2014. Nutrient transport through estuaries: The importance of the estuarine geography. Estuar. Coast. Shelf Sci. https://doi.org/10.1016/j.ecss.2014.03.014.
Justić, D., Rabalais, N.N., Turner, R.E., 1995. Stoichiometric nutrient balance and origin of coastal eutrophication. Mar. Pollut. Bull. 30, 41–46.
Kanakidou, M., Duce, R.A., Prospero, J.M., Baker, A.R., Benitez-Nelson, C., et al., 2012. Atmospheric fluxes of organic N and P to the global ocean. Glob. Biogeochem. Cycles 26, GB3026. https://doi.org/10.1029/2011GB004277.
Kanakidou, M., Myriokefalitakis, S., Tsigaridis, K., 2018. Aerosols in atmospheric chemistry and biogeochemical cycles of nutrients. Environ. Res. Lett. 13 (6), 063004 https://doi.org/10.1088/1748-9326/aabcdb.
Khammeri, Y., Hamza, I., Zouari, A., Hamza, A., Sahli, E., et al., 2018. Atmospheric bulk deposition of dissolved nitrogen, phosphorus and silicate in the Gulf of Gabès (South Ionian Basin); implications for marine heterotrophic prokaryotes and ultraphytoplankton. Cont. Shelf Res. https://doi.org/10.1016/j.csr.2018.03.003.
Khélifi-Touhami, M., Ounissi, M., Saker, I., Haridi, A., Djorfi, S., Abdenour, C., 2006. The hydrology of the Mafragh estuary (Algeria): transport of inorganic nitrogen and phosphorus to the adjacent coast. J. Food Agri. Environ. 4 (2), 340–346.
Koçak, M., Kubilay, N., Tuğrul, S., Mihalopoulos, N., 2010. Atmospheric nutrient inputs to the northern Levantine basin from a long-term observation: Sources and comparison with riverine inputs. Biogeosciences 7 (12), 4037–4050. https://doi.org/10.5194/bg-7-4037-2010.
Krom, M.D., Kress, N., Berman-Frank, I., Rahav, E., 2014. Past, present and future patterns in the nutrient chemistry of the eastern Mediterranean. In: Goffredo, S., Dubinsky, Z. (Eds.), The Mediterranean Sea. Its history and present challenges. Springer, Dordrecht, Netherlands, pp. 49–68.
Kubilay, N., Nickovic, S., Moulin, C., Dulac, F., 2000. An illustration of the transport and deposition of mineral dust onto the eastern Mediterranean. Atmos. Environ. 34, 1293–1303.
Lazzari, P., Solidoro, C., Ibello, V., Salon, S., Teruzzi, A., Beranger, K., Colella, S., Crise, A., 2012. Seasonal and inter-annual variability of plankton chlorophyll and primary production in the Mediterranean Sea: A modeling approach. Biogeosciences 9, 217–233. https://doi.org/10.5194/bg-9-217-2012.
Li, J., Fang, Y., Yoh, M., Wang, X., Wu, Z., Kuang, Y., Wen, D., 2012. Organic nitrogen deposition in precipitation in metropolitan Guangzhou city of southern China. Atmos. Res. 113, 57–67. https://doi.org/10.1016/j.atmosres.2012.04.019.
Lionello, P., Gacic, A.F., Planton, M., Trigo, S.R., Ulbrich, U., 2014. The climate of the Mediterranean region: Research progress and climate change impacts. Reg. Environ. Chang. 14, 1679–1684.
Loÿe-Pilot, M.D., Martin, M., Morelli, J., 1986. Influence of Saharan dust on the rain acidity and atmospheric input to the Mediterranean. Nature 321, 427–428.
Loÿe-Pilot, M.D., Martin, J.M., Morelli, J., 1990. Atmospheric input of inorganic nitrogen to the western Mediterranean. Biogeochemistry 9 (2), 117–134. https://doi.org/10.1007/bf00692168.
Ludwig, W., Dumont, E., Meybeck, M., Heussner, S., 2009. River discharges of water and nutrients to the Mediterranean and Black Sea: Major drivers for ecosystem changes during past and future decades? Prog. Oceanogr. 80 (3–4), 199–217. https://doi.org/10.1016/j.pocean.2009.02.001.
Maavara, T., Dürr, H.H, Van Cappellen, P., 2014. Worldwide retention of nutrient silicon by river damming: from sparse data set to global estimate. Glob. Biogeochem. Cy. 28, 842–855.
Mace, K.A., Kubilay, N., Duce, R.A., 2003. Organic nitrogen in rain and aerosol in the eastern Mediterranean atmosphere: An association with atmospheric dust. J. Geoph. Res.: Atmosph. 108 (D10), 4320.
Macias, D., Garcia-Gorriz, E., Stips, A., 2017. Major fertilization sources and mechanisms for Mediterranean Sea coastal ecosystems. Limnol. Oceanogr. 63, 897–914. https://doi.org/10.1002/lno.10677.
Malago, A., Bouraoui, F., Grizzetti, B., De Roo, A., 2019. Modelling nutrient fluxes into the Mediterranean Sea. J. Hydrol. 22, 100592. https://doi.org/10.1016/j.ejrh.2019.01.004.
Markaki, Z., Oikonomou, K., Koçak, M., Kouvarakis, G., Chaniotaki, A., Kubilay, N., Mihalopoulos, N., 2003. Atmospheric deposition of inorganic phosphorus in theLevantine Basin, eastern Mediterranean: Spatial and temporal variability and its role in seawater productivity. Limnol. Oceanogr. 48 (4), 1557–1568. https://doi.org/10.4319/lo.2003.48.4.1557.
Markaki, Z., Loÿe-Pilot, M.D., Violaki, K., Benyahya, L., Mihalopoulos, N., 2010. Variability of atmospheric deposition of dissolved nitrogen and phosphorus in theMediterranean and possible link to the anomalous seawater N/P ratio. Mar. Chem. 120 (1), 187–194. https://doi.org/10.1016/j.marchem.2008.10.005.
Martin, J.M., Elbaz-Poulichet, F., Guieu, C., Loÿe-Pilot, M.D., Han, G., 1989. River versus atmospheric input of material to the Mediterranean Sea: An overview. Mar. Chem. 28 (1–3), 159–182. https://doi.org/10.1016/0304-4203(89)90193-X.
Medinets, S., Medinets, V., 2012. Investigations of atmospheric wet and dry nutrient deposition to marine surface in western part of the Black Sea. Turk. J. Fish. Aqua. Sci. 12, 497–505.
Mehta, A.V., Yang, S., 2008. Precipitation climatology over Mediterranean Basin from ten years of TRMM measurements. Adv. Geosci. 17, 87–91. https://doi.org/10.5194/adgeo-17-87-2008.
Milliman, J.D., 2001. River inputs. In: Steele, J.H., Turekian, K.K.A., Thorpe, S.A. (Eds.), Encyclopedia of Ocean Sciences, vol. 4. Academic Press, pp. 2419–2427. https://doi.org/10.1006/rwos.2001.0074.
Moon, J.-Y., Lee, K., Tanhua, T., Kress, N., Kim, I.-N., 2016. Temporal nutrient dynamics in the Mediterranean Sea in response to anthropogenic inputs. Geophys. Res. Lett. 43, 5243–5251. https://doi.org/10.1002/2016gl068788.
Morales-Baquero, R., Pulido-Villena, E., Reche, I., 2013. Chemical signature of Saharan dust on dry and wet atmospheric deposition in the south-western Mediterranean region. Tellus B: Chem. Phys. Meteorol. 65 (1), 1–11. https://doi.org/10.3402/tellusb.v65i0.18720.
Mörth, C.-M., Humborg, C., Eriksson, H., Danielsson, A., Medina, M.R., Löfgren, S., Dennis, P., Swaney, D.P., Rahm, L., 2007. Modelling riverine nutrient transport to the Baltic Sea-a large-scale approach. Ambio 36 (2), 124–133. https://doi.org/10.1579/0044-7447(2007)36[124:MRNTTT]2.0.CO;2.
Neff, J.C., Holland, E.A., Dentener, F.J., McDowell, W.H., Russell, K.M., 2002. The origin, composition and rates of organic nitrogen deposition: A missing piece of the nitrogen cycle? Biogeochemistry 57 (58), 99–136.
Nehir, M., Koçak, M., 2018. Atmospheric water-soluble organic nitrogen (WSON) in the Eastern Mediterranean: Origin and ramifications regarding marine productivity. Atmos. Chem. Phys. 18, 3603–3618. https://doi.org/10.5194/acp-18-3603-2018.
Ounissi, M., Bouchareb, N., 2013. Nutrient distribution and fluxes from three Mediterranean coastal rivers (NE Algeria) under large damming. CR Geosci. 345 (2), 81–92. https://doi.org/10.1016/j.crte.2013.02.002.
Ounissi, M., Frehi, H., 1999. Variability of microphytoplankton and Tintinnida (ciliated protozoa) in an eutrophic sector of the Annaba Gulf (S.W. Mediterranean). Cah. Biol. Mar. 40 (2), 141–153.
Ounissi, M., Frehi, H., Khelifi-Touhami, M., 1998. Composition et abondance du zooplancton en situation d'eutrophisation dans un secteur côtier du golfe d'Annaba (Algérie). Ann. Inst. Océanogr. 74, 13–28.
Ounissi, M., Ziouch, O.R., Aounallah, O., 2014. Variability of the dissolved nutrient (N, P, Si) levels in the Bay of Annaba in relation to the inputs of the Seybouse and Mafragh estuaries. Mar. Pollut. Bull. 80 (1), 234–244. https://doi.org/10.1016/j.marpolbul.2013.12.030.
Ounissi, M., Laskri, H., Khélifi-Touhami, M., 2016. Net-zooplankton abundance and biomass from Annaba Bay (SW Mediterranean Sea) under estuarine influences. Medit. Mar. Sci. 17 (2), 519–532. https://doi.org/10.12681/mms.1474.
Ounissi, M., Amira, A.B., Dulac, F., 2018. Riverine and wet atmospheric inputs of materials to a North Africa coastal site (Annaba Bay, Algeria). Prog. Oceanogr. 165, 19–34. https://doi.org/10.1016/j.pocean.2018.04.001.
Parsons, T.R., Maita, Y., Lalli, C.M., 1989. A Manual of Chemical and Biological Methods for Sea Water Analysis. Pergamon Press, Oxford.
Peixoto, J.P., De Almeida, M., Rosen, R.D., Salste, D.A., 1982. Atmospheric moisture transport and the water balance of the Mediterranean Sea. Water Resour. Res. 18 (1), 83–90.
Philandras, C.M., Nastos, P.T., Kapsomenakis, J., Douvis, K.C., Tselioudis, G., Zerefos, C. S., 2011. Long-term precipitation trends and variability within the Mediterranean region. Nat. Hazards Earth Syst. Sci. 11, 3235–3250. https://doi.org/10.5194/nhess-11-3235-2011.
Powley, H.R., Krom, M.D., Van Cappellen, P., 2017. Understanding the unique biogeochemistry of the Mediterranean Sea: Insights from a coupled phosphorus and nitrogen model. Glob. Biogeochem. Cycles 31, 1010–1031. https://doi.org/10.1002/2017GB005648.
Preston, S.D., Bierman, J.R.V.J., Silliman, S.E., 1989. An evaluation of methods for the estimation of tributary mass loads. Water Resour. Res. 25 (6), 1379–1389.
Prospero, J.M., 2014. Characterizing the temporal and spatial variability of African dust over the Atlantic. PAGES Magazine 22 (2), 12–13.
Prospero, J.M., Ginoux, P., Torres, O., Nicholson, S.E., Gill, T.E., 2002. Environmental characterization of global sources of atmospheric soil dust identified with the Nimbus 7 Total Ozone Mapping Spectrometer (TOMS) absorbing aerosol product. Rev. Geophys. 40 (1), 1002. https://doi.org/10.1029/2000RG000095.
Rendell, A.R., Ottley, C.J., Jickells, T.D., Harrison, R.M., 1993. The atmospheric input of nitrogen species to the North Sea. Tellus B: Chem. Phys. Meteorol. 45 (1), 53–63.
Ridame, C., Guieu, C., 2002. Saharan input of phosphate to the oligotrophic water of the open western Mediterranean Sea. Limnol. Oceanogr. 47 (3), 856–869. https://doi.org/10.4319/lo.2002.47.3.0856.
Rogora, M., Mosello, R., Marchetto, A., 2004. Long-term trends in the chemistry of atmospheric deposition in northwestern Italy: The role of increasing Saharan dust deposition. Tellus B 56 (5), 426–434.
Rolff, C., Elmgren, R., Voss, M., 2008. Deposition of nitrogen and phosphorus on the Baltic Sea: Seasonal patterns and nitrogen isotope composition. Biogeosciences 5, 1657–1667. https://doi.org/10.5194/bg-5-1657-2008.
Romero, E., Garnier, J., Lassaletta, L., Billen, G., Le Gendre, R., Riou, P., Cugier, P., 2013. Large-scale patterns of river inputs in southwestern Europe: Seasonal and interannual variations and potential eutrophication effects at the coastal zone. Biogeochemistry 113 (1–3), 481–505. https://doi.org/10.1007/s10533-012-9778-0.

Salvador, P., Alonso-Pérez, S., Pey, J., Artíñano, B., de Bustos, J.J., Alastuey, A., Querol, X., 2014. African dust outbreaks over the western Mediterranean Basin: 11-year characterization of atmospheric circulation patterns and dust source areas. Atmos. Chem. Phys. 14, 6759–6775. https://doi.org/10.5194/acp-14-6759-2014.

Skoulikidis, T.N., Sabater, S., Datry, T., Morais, M.A., Buffagni, A., et al., 2016. Non-perennial Mediterranean rivers in Europe: Status, pressures, and challenges for research and management. Sci. Total Environ. 557, 1–18. https://doi.org/10.1016/j.scitotenv.2016.10.147.

Song, J., 2011. Biogeochemical Processes of Biogenic Elements in China Marginal Seas. Springer Science and Business Media.

Struglia, M.V., Mariotti, A., Filograsso, A., 2004. River discharge into the Mediterranean Sea: Climatology and aspects of the observed variability. J. Clim. 17, 4740–4751. https://doi.org/10.1175/JCLI-3225.1.

Sugimoto, R., Tsuboi, T., 2017. Seasonal and annual fluxes of atmospheric nitrogen deposition and riverine nitrogen export in two adjacent contrasting rivers in central Japan facing the sea of Japan. J. Hydrol. Reg. Stud. 11, 117–125. https://doi.org/10.1016/j.ejrh.2015.11.019.

Tarolli, P., Borga, M., Morin, E., Delrieu, G., 2012. Analysis of flash flood regimes in the North-Western and South-Eastern Mediterranean regions. Nat. Hazards Earth Syst. Sci. 12, 1255–1265. https://doi.org/10.5194/nhess-12-1255-2012.

Tong, Y., Zhao, Y., Zhen, G., Chi, J., Liu, X., Lu, Y., Zhang, W., 2015. Nutrient loads flowing into coastal waters from the main rivers of China (2006-2012). Sci. Rep. 5, 16678. https://doi.org/10.1038/srep16678.

Tovar-Sánchez, A., Basterretxea, G., Ben Omar, M., Jordi, A., SánchezQuiles, D., Makhani, M., Mouna, D., Muya, C., Anglès, S., 2016. Nutrients, trace metals and B-vitamin composition of the Moulouya River: A major North African river discharging into the Mediterranean Sea. Estuar. Coast. Shelf Sci. https://doi.org/10.1016/j.ecss.2016.04.006.

Treguer, P., Nelson, D.M., Van Bennekom, A.J., DeMaster, D.J., Leynaert, A., Queguiner, B., 1995. The silica balance in the World Ocean: a reestimate. Science 268 (5209), 375–379.

Turner, R.E., Qureshi, N., Rabalais, N.N., Dortch, Q., Justic, D., Shaw, R.F., Cope, J., 1998. Fluctuating silicate: Nitrate ratios and coastal plankton food webs. Proc. Natl. Acad. Sci. 95 (22), 13048–13051.

Ulbrich, U., Lionello, P., Belusic, D., Jacobeit, J., Knippertz, P., Kuglitsch, F.G., et al., 2012. Climate of the Mediterranean: synoptic patterns, temperature, precipitation, winds, and their extremes. In: Lionello, P., et al. (Eds.), The climate of the Mediterranean region: From the past to the future. Elsevier, pp. 301–346. https://doi.org/10.1016/B978-0-12-416042-2.00005-7.

UNEP/MAP/MED POL Report, 2013. Rivers of the Mediterranean Sea: Water discharge and nutrient fluxes. UNEP/MAP, MED POL CEFREM 30.

Varga, G., Újvári, G., Kovács, J., 2014. Spatiotemporal patterns of Saharan dust outbreaks in the Mediterranean Basin. Aeolian Res. 15, 151–160. https://doi.org/10.1016/j.aeolia.2014.06.005.

Viaroli, P., Daniele, N., Pinardi, M., Soana, E., Bartoli, M., 2015. Eutrophication of the Mediterranean Sea: A watershed-cascading aquatic filter approach. Rend. Fis. Acc. Lincei. 26, 13–23. https://doi.org/10.1007/s12210-014-0364-3.

Vincent, J., Laurent, B., Losno, R., Bon Nguyen, E.B., Roullet, P., et al., 2016. Variability of mineral dust deposition in the western Mediterranean basin and south-east of France. Atmos. Chem. Phys. 16, 8749–8766. https://doi.org/10.5194/acp-16-8749-2016.

Violaki, K., Zarbas, P., Mihalopoulos, N., 2010. Long-term measurements of dissolved organic nitrogen (DON) in atmospheric deposition in the eastern Mediterranean: fluxes, origin and biogeochemical implications. Mar. Chem. 120 (1–4), 179–186. https://doi.org/10.1016/j.marchem.2009.08.004.

Wang, F., Polcher, J., 2019. Assessing the freshwater flux from the continents to the Mediterranean Sea. Sci. Rep. 9 (1) https://doi.org/10.1038/s41598-019-44293-1.

Xoplaki, E., Trigo, R.M., Garcı'a-Herrera, R.F., Barriopedro, D., D'Andrea, F., et al., 2014. Large-scale atmospheric circulation driving extreme climate events in the Mediterranean and its related impacts. In: Lionello, P., et al. (Eds.), The climate of the Mediterranean region: From the past to the future. Elsevier, pp. 347–417. https://doi.org/10.1016/B978-0-12-416042-2.00006-9.

Yool, A., Tyrrell, T., 2003. Role of diatoms in regulating the ocean's silicon cycle. Glob. Biogeochem. Cycles 17 (4), 1103. https://doi.org/10.1029/2002GB002018.

Zhang, Y., Song, L., Liu, X.J., Li, W.Q., Lü, S.H., Zheng, L.X., Bai, Z.C., Cai, G.Y., Zhang, F. S., 2012. Atmospheric organic nitrogen deposition in China. Atmos. Environ. 46, 195–204. https://doi.org/10.1016/j.atmosenv.2011.09.080.

Ziouch, O.R., Laskri, H., Chenaker, H., Ledjedel, N.E., Daifallah, T., Ounissi, M., 2020. Transport of nutrients from the Seybouse River to Annaba Bay (Algeria, SW Mediterranean). Mar. Pollut. Bull. 156 (2020), 111231. https://doi.org/10.1016/j.marpolbul.2020.111231.